

Aus der Medizinischen Universitätsklinik  
Abteilung Innere Medizin IV  
(Nephrologie)  
der Albert-Ludwigs-Universität Freiburg im Breisgau

***C. elegans* as model organism for the identification of new  
components of the TOR signaling pathway**

INAUGURAL-DISSERTATION

zur

Erlangung des Medizinischen Doktorgrades  
der Medizinischen Fakultät  
der Albert-Ludwigs-Universität  
Freiburg im Breisgau

Vorgelegt 2010

von Raquel Guerola Segura  
geboren in Sevilla, Spanien

Dekan: Prof. Dr. Dr. h.c. mult. Hubert Erich Blum  
Erster Gutachter: Prof. Dr. Gerd Walz  
Zweiter Gutachter: Prof. Dr. Hans-Georg Koch

Jahr der Promotion: 2011

# Index

<b>1. Summary / Zusammenfassung</b> .....	1
<b>2. Introduction</b> .....	3
2.1 Polycystic kidney disease .....	3
2.1.1 Autosomal dominant polycystic kidney disease: an overview .....	3
2.1.2 Molecular genetics of ADPKD.....	4
2.1.3 The role of mTOR in polycystic kidney disease .....	5
2.2 Mammalian target of rapamycin (mTOR) signaling pathway .....	6
2.2.1 mTOR complexes.....	6
2.2.2 mTOR is a central determinant of growth and metabolism.....	7
2.3 The model organism <i>C. elegans</i> .....	11
2.3.1 <i>C. elegans</i> life cycle and biology .....	11
2.3.2 TOR signaling in <i>C. elegans</i> .....	13
2.4 Aim of this work.....	17
<b>3 Materials and methods</b> .....	18
3.1 Materials.....	18
3.1.1 Solutions and buffers .....	18
3.1.2 Media .....	19
3.1.3 <i>C. elegans</i> strains.....	20
3.1.4 Bacteria strains.....	20
3.1.5 Plasmids and vectors .....	21
3.2 Molecular biology methods.....	22
3.2.1 Polymerase chain reaction (PCR) .....	22
3.2.2 RNA isolation from <i>C. elegans</i> and reverse transcriptase PCR (RT-PCR).....	23
3.2.3 Cloning procedure .....	23
3.3 <i>C. elegans</i> methods.....	24
3.3.1 Breeding of <i>C. elegans</i> .....	24
3.3.10 Microscopy .....	33
3.3.2 Synchronization of <i>C. elegans</i> strains .....	25
3.3.3 Genotyping of <i>C. elegans</i> by single worm PCR .....	26
3.3.4 Microinjection of <i>C. elegans</i> .....	26
3.3.5 Crossing of <i>C. elegans</i> strains.....	27
3.3.6 RNA interference (RNAi).....	29
3.3.7 RNAi screening .....	31

3.3.8 Larval arrest test.....	32
3.3.9 Determination of <i>C. elegans</i> lifespan.....	33
<b>4. Results</b> .....	<b>34</b>
4.1 Analysis of <i>let-363/CeTOR</i> expression in <i>C. elegans</i> .....	34
4.1.1 <i>let-363/CeTOR</i> is <i>trans</i> -spliced and locates in an operon .....	34
4.1.2 Analysis of <i>let-363/CeTOR</i> transcriptional regulation and expression pattern....	36
4.1.3 The expression pattern of <i>daf-15/CeRaptor</i> resembles that of <i>let-363/CeTOR</i> . 42	
4.2 Knockdown of <i>let-363/CeTOR</i> in <i>C. elegans</i> results in a pleiotropic phenotype .....	44
4.3 Genome-wide RNAi screening for genes that modulate CeTOR function .....	47
4.3.1 Generation of a stable <i>let-363/CeTOR</i> mutant strain for RNAi screening approaches .....	47
4.3.2 Design of a genome-wide RNAi screen for genes interacting with CeTOR to regulate larval development .....	50
4.4 Identification of a new CeTOR regulator: <i>MST1 C. elegans</i> orthologue <i>cst-1</i> modulates <i>let-363/CeTOR</i> .....	53
4.4.1 Knockdown of <i>cst-1</i> partially suppresses <i>let-363</i> L3-arrest phenotype .....	54
4.4.2 Knockout of <i>cst-1</i> suppresses <i>let-363</i> extended lifespan phenotype .....	55
<b>5. Discussion</b> .....	<b>57</b>
5.1 Expression analysis of <i>let-363/CeTOR</i> .....	57
5.1.1 <i>let-363/CeTOR</i> locates in an operon and is expressed together with and downstream of the mitochondrial ribosomal protein B0261.4 .....	57
5.1.2 <i>let-363/CeTOR</i> is strongly expressed in tissues that regulate development through sensing the nutritional status .....	58
5.2 Search for CeTOR genetic interactors by genome-wide RNAi screening .....	60
5.3 <i>let-363/CeTOR</i> interacts with <i>cst-1</i> , the <i>C. elegans</i> orthologue of <i>MST1</i> in the mammalian Hippo pathway.....	61
5.4 Conclusions.....	63
<b>6. Appendix</b> .....	<b>64</b>
<b>7. Abbreviations</b> .....	<b>65</b>
<b>8. References</b> .....	<b>67</b>
<b>9. Acknowledgements</b> .....	<b>74</b>
<b>10. Curriculum Vitae</b> .....	<b>75</b>

## 1. Summary

Autosomal dominant polycystic kidney disease (ADPKD) is a frequent systemic disorder characterized by the development of renal cysts leading to end-stage renal failure. Recently, the pathogenesis of renal cyst formation and progression of PKD has been linked to mammalian target of rapamycin (mTOR). Dysregulation of mTOR may represent a common final pathway in cystogenesis. However, the underlying events causing mTOR activation are poorly understood.

In this project, the model organism *C. elegans* was used to investigate the regulation and function of TOR signaling *in vivo*. In the nematode, CeTOR is a central regulator of development and longevity, and reduction of CeTOR activity results in larval developmental arrest and increased lifespan.

We first analyzed the transcriptional regulation and expression pattern of *CeTOR*. Here we demonstrated that *CeTOR* locates in an operon (a gene cluster) downstream of a gene coding for a ribosomal protein, suggesting the co-regulation of these proteins. Using GFP-reporter constructs driven by different parts of *CeTOR* upstream regulatory regions we determined the expression pattern of CeTOR. In agreement with its broad functions, we observed expression in head and tail neurons, hypodermis, pharynx, and intestine throughout all stages of postembryonic development and adulthood. Moreover, we showed that regulatory sequences contained in the upstream gene of the operon are essential for robust *CeTOR* expression, and that different segments of the promoter confer expression in different tissues.

Next, we designed a genome-wide RNAi screening approach to search for factors modulating CeTOR function. For this purpose, we generated a balanced *CeTOR*-mutant strain and established an optimized screening protocol. The experimental setup described here will provide a novel approach for identifying and validating regulators involved in TOR signaling.

Finally, we identified a genetic interaction between *CeTOR* and *cst-1*, the *C. elegans* orthologue of MST1 of the Hippo pathway. Knockdown of *cst-1* partially reversed the larval arrest and suppressed the extended lifespan derived from *CeTOR* loss of function, supporting a model in which both pathways antagonistically interact to control development and longevity.

These approaches present the nematode *C. elegans* as a very versatile tool to study the genetic basis of TOR signaling and connected signaling cascades.

## Zusammenfassung

Die autosomal dominante polyzystische Nierenerkrankung ist eine häufige Systemerkrankung, die mit der Entwicklung von Nierenzysten einhergeht und zur terminalen Niereninsuffizienz führt. Kürzlich wurde der *mammalian target of Rapamycin (mTOR)* Signalweg mit der Pathogenese der Zystenbildung und Progression der polyzystischen Nierenerkrankung in Verbindung gebracht. Welche Ereignisse zur Aktivierung des *mTOR* Signalweges führen sind jedoch bislang unzureichend geklärt.

In dieser Arbeit wurde die Funktion und Regulation des *TOR*-Signalweges im Modellorganismus *C. elegans* untersucht. In *C. elegans* ist *CeTOR* entscheidend an der Regulation von Entwicklungs- und Alterungsprozessen beteiligt. So führt die Reduktion der *CeTOR*-Aktivität zur Entwicklungshemmung im Larvenstadium und verlängerter Lebensdauer.

Zunächst wurden die transkriptionelle Regulation und das Expressionsmuster von *let-363/CeTOR* untersucht. Es konnte gezeigt werden, dass *CeTOR* downstream von einem Gen, das für ein ribosomales Protein kodiert, in einem Gencluster (sogenanntem Operon) liegt, was darauf hindeutet, dass diese Proteine gemeinsam reguliert werden. Das detaillierte Expressionsmuster von *CeTOR* wurde mittels GFP-Reporterkonstrukten bestimmt, die unterschiedlichen Promoterregionen enthielten. *CeTOR* wurde in Kopf- und Schwanzneuronen, der Hypodermis, dem Pharynx und dem Darm während allen Entwicklungsstadien sowie im adulten Wurm exprimiert, was vereinbar ist mit den vielfältigen Funktionen von *CeTOR*. Zusätzlich konnte gezeigt werden, dass Sequenzabschnitte in dem upstream von *let-363/CeTOR* gelegenen Gen entscheidend sind für eine stabile Expression von *CeTOR*. Außerdem steuern unterschiedliche Abschnitte des Promoters die Expression von *CeTOR* in unterschiedlichen Geweben.

Ein besonderer Schwerpunkt dieser Arbeit war die Entwicklung eines *RNAi-Screens* zur genomweiten Suche nach Faktoren, die *CeTOR* funktionell modulieren. Hierfür wurde eine *let-363* Mutante generiert, in der die letale Mutation balanciert war, und ein *RNAi*-Protokoll etabliert und optimiert. Mit diesem experimentellen Versuchsaufbau wird es möglich sein, neue Regulatoren des *TOR*-Signalweges zu identifizieren und zu validieren.

Außerdem wurde eine genetische Interaktion zwischen *CeTOR* und *cst-1*, dem *C. elegans* Ortholog von MST1 aus dem Hippo-Signalweg, identifiziert. Durch Reduktion der *cst-1* Aktivität konnte die Verzögerung der *CeTOR* Larvenentwicklung teilweise aufgehoben werden. Ebenso wurde die verlängerte Lebensdauer von *CeTOR* durch Mutation von *cst-1* supprimiert. Anhand dieser Daten kann ein Modell entwickelt werden, in dem beide Signalwege Entwicklungs- und Alterungsprozesse antagonistisch steuern.

Das hier beschriebene *C. elegans*-Modellsystem bietet einen neuartigen Ansatz, um die genetische Grundlagen des *TOR*-Signalweges und die Verbindung zu anderen Signalkaskaden zu analysieren.

## 2. Introduction

### 2.1 Polycystic kidney disease

Polycystic kidney disease (PKD) is a group of inherited disorders characterized by morbidity-associated development of renal cysts. A large variety of diseases with different modes of inheritance, presentation and severity cause polycystic kidneys, most of them associated with extrarenal manifestations. Mutations in more than 20 genes have been identified that cause PKD. Most of the proteins involved in PKD pathogenesis have been localized to primary cilium or its base, the basal body, and abnormalities of cilia in the kidney are associated with cysts development. Autosomal dominant polycystic kidney disease (ADPKD) is by far the most prevalent form of PKD (28).

#### 2.1.1 Autosomal dominant polycystic kidney disease: an overview

Autosomal dominant polycystic kidney disease (ADPKD) is one of the most common inherited disorders in humans, affecting one in 500-1,000 people. It is the most common genetic cause of renal failure and accounts for up to 10% of all patients with end-stage renal disease. Mutations in *PKD1* are responsible for 85% of the cases (ADPKD1), while defects in *PKD2* underlie 15% of the cases (ADPKD2). Although both produce identical clinical manifestation, ADPKD2 has a milder course (28, 90).

In ADPKD, cysts arise in both kidneys from different segments of the nephron. They enlarge progressively through proliferation and accumulation of cyst fluid, eventually disconnecting from the rest of the renal tubule, and destroy the surrounding tissue by expansion. Consequently, there is progressive bilateral kidney enlargement and loss of renal function (28, 90).

ADPKD patients often remain asymptomatic until middle or late adulthood, and renal failure usually occurs during the fifth or sixth decade of life. Typical renal manifestations include arterial hypertension, flank or abdominal pain, hematuria, nephrolithiasis and recurrent urinary tract infections. ADPKD is a systemic disorder associated with extrarenal abnormalities, such as cerebral and abdominal aneurysms, cardiac valvular defects, colon diverticulosis and cysts development in liver, spleen and pancreas (6, 28, 90).

Diagnosis is mainly based on imaging techniques (ultrasonography, CT or MR) and family anamnesis (positive for ADPKD in approximately 70% of the cases). However, it is important to perform differential diagnosis with other PKD disorders. Given the correlation between renal structure and functional changes, renal volume measurements can be used to monitor disease progression before reaching a relevant decline in function (6, 90).

Current management of ADPKD is directed to alleviation of symptoms and limitation of the complications of hypertension and renal failure (6, 56). However, new discoveries in the field of PKD pathophysiology have facilitated the development of several new promising therapeutic approaches. Among others, there are already ongoing clinical trials of vasopressin-2-receptor antagonists (tolvaptan), somatostatin analogues (octreotide, lanreotide) and mammalian target of rapamycin (mTOR) inhibitors (sirolimus, everolimus) (90).

### **2.1.2 Molecular genetics of ADPKD**

Mutations in at least two different genes, *PKD1* and *PKD2*, account for ADPKD. Polycystin-1 (PC1), encoded by *PKD1*, is a large integral membrane protein with the overall structure of a receptor or adhesion molecule. It contains a long N-terminal extracellular domain, 11 transmembrane domains and a short cytoplasmic C-terminus (32, 73). Polycystin-2 (PC2), encoded by *PKD2*, is a non-selective cation channel with a preference for calcium. It consists of six transmembrane domains and intracellular N- and C-terminus (22, 60). PC1 interacts with PC2 via its cytoplasmic domain to form a heterodimeric complex (69, 92). Most remarkably, both colocalize in the renal cilium, a long non-motile microtubule-based projection in the apical surface of tubular epithelial cells that extends into the lumen of the tubule (101).

It has been hypothesized that the polycystin complex acts as mechanosensor of luminal flow on cilia. Flow-induced bending of the cilium is detected by PC1, which activates PC2. This leads to a calcium influx into the cell occurring through the PC2 channel (61, 62). Consistent with the polycystin complex having a role in calcium regulation, PKD cells display altered intracellular calcium homeostasis (1).

The pathways regulated by this influx of calcium constitute a very intricate network not completely understood, but it seems clear that they are necessary for normal kidney development. Disruption of primary renal cilia, as well as loss of function or



low expression of either PC1 or PC2, leads to cellular dedifferentiation, uncontrolled proliferation and cysts development (16, 38, 100). However, overexpression of PKD1 has been found to cause PKD in mice, suggesting gain of function could also have a role on cystogenesis (88).

### **2.1.3 The role of mTOR in polycystic kidney disease**

Recently, the protein mammalian target of rapamycin (mTOR) has been linked to the pathogenesis of renal cyst formation and disease progression in PKD. mTOR is a central controller of cell growth and growth-related processes, such as proliferation, metabolism and autophagy (98, 99). Treatment with rapamycin, a specific mTOR inhibitor, has been proved effective in several rodent models of PKD, where it was able to reduce cyst and kidney volumes and slow the progression of the disease (77, 78, 87, 94). In addition, retrospective studies of transplant-recipient ADPKD patients who received mTOR inhibitors as immunosuppressive agents showed a reduction in size of the native polycystic kidneys and liver (70, 77). In agreement with these findings, it has been reported that epithelial cells lining cysts of polycystic kidneys exhibit increased mTOR activity (77). Taken together, these observations support the hypothesis that dysregulation of mTOR activity plays a major role in PKD pathophysiology. However, upstream events activating mTOR in the tubular epithelium and their relation to altered ciliary function are poorly understood.

One important negative regulator of mTOR is the TSC complex, formed of hamartin (TSC1) and tuberlin (TSC2) (98). Mutations in *TSC1* and *TSC2* lead to tuberous sclerosis, a multisystemic disease included in the PKD group characterized by renal cysts and multiple benign tumors in different organs (50). Patients with mutations in both *PKD1* and *TSC2* suffer from a very severe form of PKD, suggesting a synergistic effect of both pathways in cystogenesis (11). This hypothesis was supported by the finding that the cytoplasmic tail of PC1 directly interacts with tuberlin (77). Very recently, it has been demonstrated that PC1 protects tuberlin from being phosphorylated and inactivated by Akt (see below), thus, retaining tuberlin at the membrane, where it remains active and able to repress mTOR signaling (17).

The increasing experimental evidence of mTOR playing an important role in the pathogenesis of ADPKD together with the promising results in PKD model animals have made the mTOR pathway a potential target for intervention. Furthermore, there

are currently several clinical trials in progress testing rapamycin and its analogue everolimus in ADPKD patients (90, 95).

## 2.2 Mammalian target of rapamycin (mTOR) signaling pathway

### 2.2.1 mTOR complexes

Mammalian target of rapamycin (mTOR) is a highly conserved protein kinase named after its specific inhibitor rapamycin, a potent anti-fungal macrolide first discovered on the Easter Island, also called Rapa Nui. mTOR was immediately related to many essential biological processes, such as cell growth, proliferation and metabolism. A TOR homologue has been identified in every genome examined until now and its disruption is lethal in all analyzed species (3, 98, 99).

mTOR is an atypical serine/threonine protein kinase of the phosphatidylinositol kinase-related kinase (PIKK) family. It is a large protein with many protein-protein interaction domains (Fig. 1) (99).

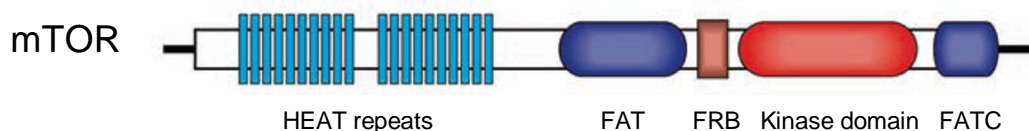


Figure 1. Schematic representation of mTOR structure. HEAT: a protein-protein interaction structure. FAT: a domain structure also found in other members of the PIKK family. FRB: FKBP12/rapamycin binding domain. FATC: C-terminal FAT domain. Source: Qian Yang, Kun-Liang Guan (99); modified.

mTOR signals through two functionally distinct multiprotein complexes: mTORC1 and mTORC2. Both complexes share mTOR and mLST8, and contain complex-specific components, such as Raptor and PRAS40 in mTORC1, and Rictor, Proctor and mSin1 in mTORC2 (3). Recently, DEPTOR has been identified as a new interactor and inhibitor of both mTOR complexes (65). Rapamycin directly binds and inhibits mTORC1 but not mTORC2, which is rapamycin insensitive (53).

mTORC1 operates as a central positive regulator of cell growth and proliferation by modulating many important cellular processes, like protein synthesis and autophagy (98). In this complex, Raptor is mainly responsible for substrate recognition and

presentation, and has an essential role in the activation of downstream targets. It has also been suggested that Raptor stabilizes mTOR and may be related to diverse stimuli affecting mTOR, such as nutrient deprivation. Knockout of Raptor, like mTOR knockout, is embryonic lethal, indicating that Raptor is indispensable for the correct function of mTORC1 (27, 43, 63). The precise role of mLST8 is still not known. Some studies suggest that mLST8 is necessary for full catalytic activity of mTOR, but others show that it is dispensable for mTORC1 function (23, 44). Rapamycin, in complex with the small binding protein FBPK12, binds to the FRB domain of mTOR and specifically inhibits its function exclusively in mTORC1. The inhibition mechanisms are not clear yet, but it seems like FKBP12/rapamycin blocks the interaction of mTORC1 with its substrates by dissociating Raptor from mTORC1. Furthermore, it directly inhibits mTOR autophosphorylation and, therefore, its intrinsic kinase activity mTORC1 (34, 43).

mTORC2 has been mainly associated with cell cycle-dependent regulation of cell morphology and cytoskeletal organization in a rapamycin-insensitive manner (98). Although it remains unclear how mTORC2 specifically regulates the actin cytoskeleton, recent studies show that mTORC2 phosphorylates several AGC kinases in different organisms (35). These proteins have been related to cellular growth, proliferation and survival. Another function ascribed to mTORC2 is the phosphorylation and full activation of Akt (see below), suggesting both TOR complexes might cross-talk in the regulation of cell size and cell cycle (71, 74). All mTORC2 components are essential and knockout of any of them in mice results in embryonic lethality (except for Proctor) (3).

During this project, we aimed to further investigate mTOR activity specially through mTORC1 signaling. Therefore, the upcoming information mainly refers to mTORC1.

### **2.2.2 mTOR is a central determinant of growth and metabolism**

#### *Upstream regulators*

The TOR signaling pathway integrates various intracellular and extracellular signals, such as growth factors or energy and nutrients availability, and serves as a central regulator of cell metabolism, growth, proliferation and survival. The TSC1/TSC2 complex (TSC) is the major regulator of mTORC1 signaling via negative regulation of

Rheb. TSC functions as a GTPase activating protein (GAP) towards Rheb, a small ras-like GTPase, and converts it to its inactive GDP-bound configuration. The active GTP-bound form of Rheb directly binds to mTORC1 and stimulates its kinase activity. However, the exact mechanism by which Rheb stimulates mTORC1 still remains to be determined (3, 98, 99).

Growth factors stimulate mTORC1 through activation of the PI3K/Akt cascade (Fig. 2). Binding of insulin or insulin-like growth factors (IGFs) to their receptors (IRS) triggers phosphoinositide-3-kinase (PI3K), which leads to activation of Akt. Akt directly phosphorylates and inactivates TSC2, and subsequently induces the upregulation of mTORC1 (3, 55). One important negative feedback loop comprises the mTOR target S6K1 (see below). Activation of S6K1 by mTORC1 promotes the phosphorylation of IRS1, which reduces its stability and provokes its degradation, thus, reducing the insulin/IGF signal (55, 98).

The energetic status of the cell is signaled to mTORC1 through AMP-activated kinase (AMPK). In response to energy depletion (high AMP/ATP ratio), AMPK is activated and phosphorylates TSC2, which enhances its GAP activity towards Rheb, reducing mTORC1 activation (33). Recently, AMPK has also been shown to directly inhibit mTORC1 through phosphorylation of Raptor (24).

The mechanisms by which mTOR senses the nutritional status are not clear yet. Recent studies present the Rag GTPases as mediators of nutrient-induced TOR activation independently of the TSC-Rheb axis. The Rag proteins interact with Raptor under favourable amino acid conditions. This is believed to promote the relocalization of mTORC1 to the same intracellular compartments that contain Rheb, thus, inducing TOR activation (45, 72).

In summary, mTOR integrates a variety of signals to sense when the environment is favourable for cell growth. In addition to the key signals described above, other cellular conditions and inputs have been shown to regulate mTORC1 signaling, like environmental stress, inflammation, the Wnt pathway or the Ras-ERK cascade (3, 98, 99). There is still much to understand before the complexity of the regulation of the mTOR pathway can be unravelled.

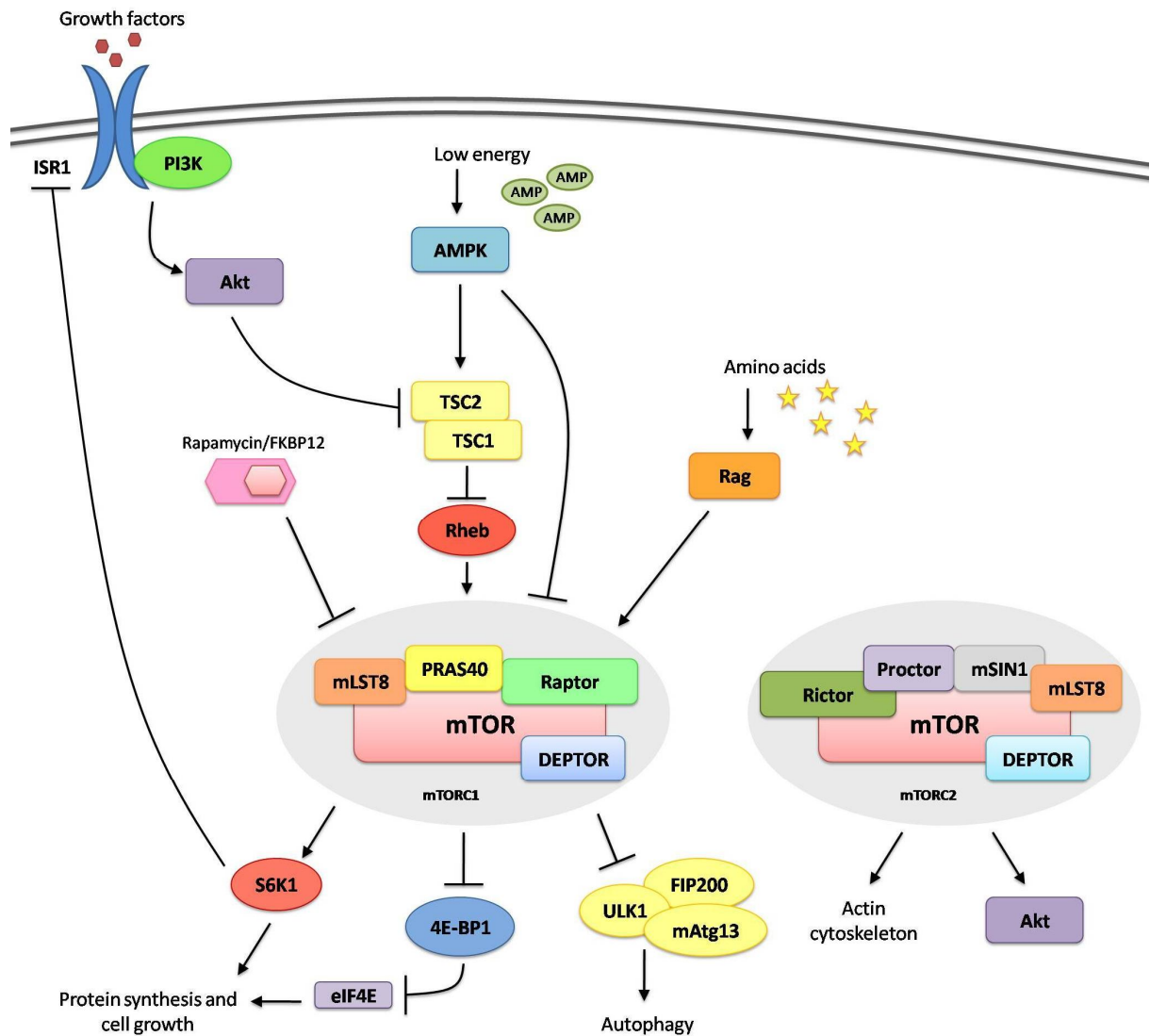


Figure 2. Schematic representation of the TOR signaling network in mammalian cells. mTOR signals through two distinct multiprotein complexes: mTORC1 (sensitive to rapamycin/FKBP12 inhibition) and mTORC2. Three major inputs are involved in the regulation of mTORC1: growth factors (insulin/IGF signaling pathway), nutritional status (amino acid availability) and energy levels (AMPK). mTORC1 modulates protein synthesis through S6K1 and 4EBP1, which are well characterized regulators of protein translation. Active S6K1 promotes attenuation of insulin/IGF signaling through inhibition of ISR1, comprising a negative feedback loop. mTORC1 also decreases autophagy through inhibition of the ULK1-mAtg13-FIP200 complex. mTORC2 regulates the actin cytoskeleton, and signals to the insulin/IGF pathway via Akt. Arrows represent activation and bars represent inhibition.

### *Downstream targets*

mTOR plays a central role on the regulation of many growth-related cellular processes by promoting anabolism, including biosynthesis of proteins, lipids and organelles, and by limiting catabolic processes, such as autophagy (98). The links between all these physiological functions are very complex and not completely understood.

The best-characterized function of mTORC1 is the control of protein synthesis by regulation of translation. Eukaryotic translation initiation factor 4E binding protein 1 (4E-BP1) and ribosomal S6 kinase 1 (S6K1) and are the major substrates of mTORC1. mTORC1 phosphorylates 4E-BP1 and, thereby, releases eIF4E, enabling it to promote translation initiation through stimulation of cap-dependent translation. Phosphorylation S6K1 by mTORC1 stimulates its activity and induces the translation of 5'TOP mRNAs, leading to increased synthesis of diverse elongation factors and ribosomal proteins (36, 55, 98). Besides, as stated above, phosphorylated S6K1 has a negative feedback effect upon the insulin-Akt signaling by promoting the degradation of the insulin receptor substrate 1 (IRS1), which in turn results in the downregulation of mTORC1 activity (55, 98). Moreover, S6K1 has been recently found to phosphorylate Rictor. This is thought to possibly reduce mTORC2 activity towards Akt, providing an additional negative feedback loop (18).

Autophagy is an important catabolic process for protein and organelle turnover. During nutrient starvation, autophagy is increased to provide nutrients from non-vital cellular components. Recent studies show that mTORC1 controls autophagy through the inhibition of the protein complex ULK1-mAtg13-FIP200, an inducer of autophagy (12). High amino acid concentration activates mTORC1 and inhibits the complex, thus, reducing autophagy, whereas starvation inhibits mTORC1 and increases this process.

## 2.3 The model organism *C. elegans*

### 2.3.1 *C. elegans* life cycle and biology

*Caenorhabditis elegans* is a free-living non-parasitic soil nematode that survives principally by feeding on bacteria. First introduced as model organism by Sydney Brenner to study neurology and genetics (10), it quickly became a very important model system thanks to its many advantages, such as its anatomic simplicity, small size, short life cycle and the numerous tools available for easy genetic and molecular manipulation. In 1998, *C. elegans* was the first multicellular organism whose genome was completely sequenced (15), and homologues have been found for approximately 64% of genes associated with human disease. This makes *C. elegans* a very powerful laboratory tool for genetic and molecular research, and so far several Nobel prizes have been awarded for investigations on *C. elegans*.

*C. elegans* adults are approximately 1 mm long. They can be easily cultivated in large quantities on Petri plates or liquid culture feeding on *E. coli*. The animals have a very simple anatomy and, since they are transparent throughout their entire life, they can be observed using diverse microscopes (Fig. 3). Wild-type adult hermaphrodites are eutelic, meaning they have a constant number of 959 somatic cells, including 302 neurons. It is known that during development exactly 131 cells undergo apoptosis. Moreover, the complete cell lineage, invariant between animals, has been mapped out, which makes the worm useful for studying cellular and organ development (84).

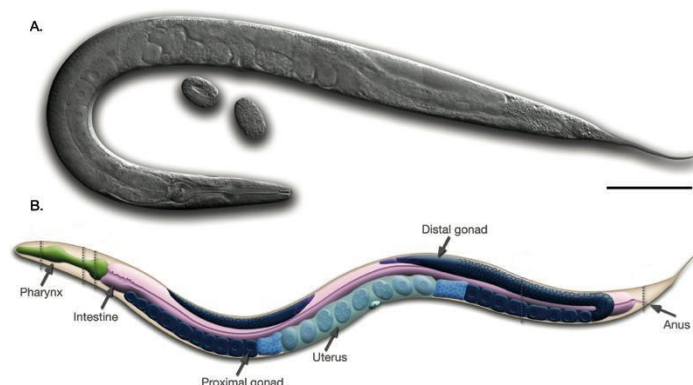


Figure 3. Anatomy of an adult *C. elegans* hermaphrodite. **A** DIC image of an adult hermaphrodite, left lateral side. Scale bar 0.1 mm. **B** Schematic drawing of anatomical structures, left lateral side. Source: <http://www.wormatlas.org>; modified.

*C. elegans* has five pairs of autosomes and one pair of sex chromosomes. It has two sexes, hermaphrodites (5AA, XX) and males (5AA, X0), the latter being only 0.1% of the population. Self-fertilization of hermaphrodites allows homozygous mutants to generate genetically identical progeny, while male mating facilitates genetic crosses. Hermaphrodites typically produce about 300 to 350 self-progeny.

Under optimal conditions, the animals have very short life cycle of about three days comprised of four larval stages (L1-L4) and adulthood, and a lifespan of approximately two to three weeks (Fig. 4). If environmental conditions are not favourable for further development at the L1-L2 stage, for example in case of food deprivation or high population density, an alternative developmental pathway is activated, and L1 larvae molt into a larval stage called “dauer”. Dauer larvae are highly stress resistant and remain viable for several months, being able to re-enter the cycle at the L4 stage if environmental conditions improve.

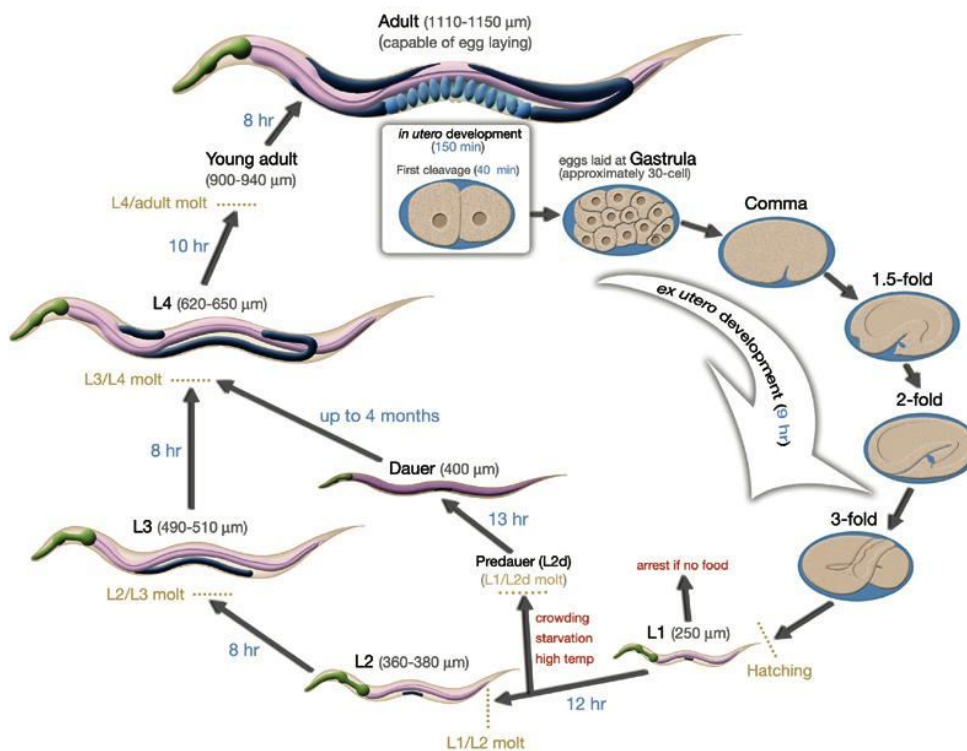


Figure 4. Life cycle of *C. elegans* at 22°C. Eggs develop in the uterus of adult hermaphrodites until laid at the 30-cell stage (gastrula). Under normal conditions, worms undergo four developmental stages, during which organogenesis is completed. L1 larvae can arrest growth after hatching in absence of food. Furthermore, under unfavourable conditions, L1 larvae can turn into dauer larvae, a highly resistant form able to survive for months. Dauer larvae can molt into L4 larvae if conditions improve. Duration of the stage and length of the animal are marked in each stage. Source: <http://www.wormatlas.org>; modified.



Despite its simplicity, *C. elegans* displays a large variety of behaviours. They are attracted to odorants and food, are repulsed by toxic chemicals, and respond to touch, light and temperature. They are also capable of highly complex functions, such as male mating, social behaviour, and learning.

One of the most remarkable features of *C. elegans* is the allowance of easy genetic manipulation. RNA-mediated interference (RNAi), microinjection and gene bombardment are widely used methods. In RNAi, double-stranded RNA is used to knock-down gene expression (20). This technique is very easy to apply, since dsRNA can be fed to the worms, and the effect is strongly and stably transmitted for generations. By microinjection or gene bombardment, methods for DNA transformation, genes can be overexpressed or ectopically expressed in many different cell types (59, 67).

### **2.3.2 TOR signaling in *C. elegans***

In *C. elegans*, TOR signaling is involved in development, metabolism and aging in response to hormone-dependent signals and nutrients. The *C. elegans* TORC1 involves LET-363/CeTOR, DAF-15/CeRaptor and LST-8 (37, 54). Absence of *let-363/CeTOR* results in different phenotypes depending on when its activity is suppressed. *let-363/CeTOR* mutants irreversibly arrest development at the L3 larval stage, display extended longevity and shift metabolism to accumulate fat, as do pre-dauer larvae (54). Inhibition of *let-363* after the L3 stage by RNAi results in developmental retardation, lifespan extension, and increased oxidative stress tolerance and fat accumulation (37, 54, 93). Similar phenotypes have been observed for inhibition of *daf-15/CeRaptor* (37).

Recently, TORC2 has been described in *C. elegans*. TORC2 functions to regulate the energetic and metabolic state of *C. elegans*, and mutations in *rict-1/CeRictor* cause increased lipid storage. Mutants are developmentally delayed and display reduced body size, fecundity and lifespan (39, 81). Interestingly, worms deprived of *lst-8* by RNAi exhibit the same phenotype as *CeRictor* mutants, and not that of *CeTOR* or *CeRaptor* (39).

### *Upstream regulators*

So far, no homologues of TSC have been found in *C. elegans*. However, an orthologue of Rheb, RHEB-1, has been recently identified. Knockdown of *rheb-1* by RNAi resulted in phenotypes similar to those of CeTOR-deficient worms (31).

There is evidence that in *C. elegans* the TOR and the insulin/IGF pathway interact at several levels to regulate development, metabolism and aging (Fig. 5). Mutations in the *C. elegans* insulin receptor *daf-2* leading to reduced insulin/IGF signaling provoke increased longevity (42, 46). This is dependent on *daf-16*, its main downstream target, which encodes the *C. elegans* orthologue of the FOXO transcription factors. Extended lifespan of *daf-2* mutants is not further increased by *let-363* knockdown, suggesting both pathways are related in controlling longevity. In addition, induction of some stress responsive genes in *let-363/CeTOR* mutants requires DAF-16. However, loss of *let-363/CeTOR* increased fat storage does not depend on DAF-16, indicating insulin-dependent and independent mechanisms of CeTOR signaling (31, 37, 93).

CeTOR has been implicated as mediator of dietary restriction-induced longevity. Dietary restriction, the limitation of food intake without malnutrition, extends lifespan from yeast to mammals. In the worm, this effect is not further increased by *let-363*RNAi, indicating dietary restriction may extend lifespan, at least in part, by downregulating CeTOR activity (26, 29). Furthermore, recent studies show that *rheb-1*RNAi mimics the effect of caloric restriction on longevity and suppresses the dietary restriction-induced extended lifespan, indicating RHEB-1 has a dual role in the regulation of fasting-induced longevity (31).

CeTOR might sense nutrients availability through amino acid transporters. The intestinal dipeptide transporter PEP-2 is involved in the absorption of dietary peptides, and its deletion enhances weak *let-363*RNAi phenotype, supporting that nutritional conditions regulate the CeTOR signaling pathway (57).

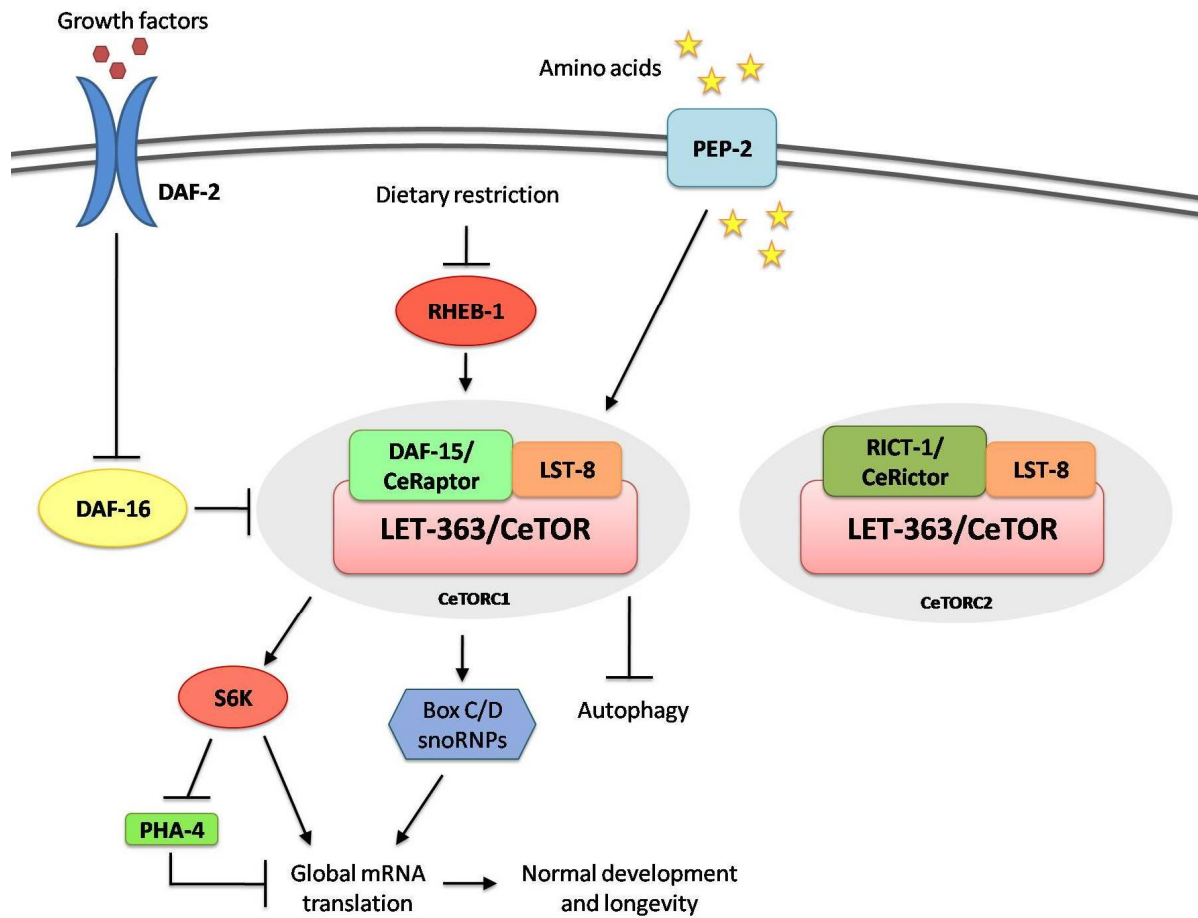


Figure 5. Proposed model of the TOR signaling network in *C. elegans*. CeTORC1 entails LET-363/CeTOR, LST-8 and DAF-15/CeRaptor, while CeTORC2 entails LET-363/CeTOR, LST-8 and RICT-1/CeRictor. CeTORC1 regulates development and longevity in response to growth factors and nutritional inputs. Growth factors activate the insulin/IGF pathway, leading to inactivation of the FOXO transcription factor DAF-16. Genetic epistasis suggests that DAF-16 acts upstream of CeTORC1 and inhibits its action. RHEB-1 and the amino acid transporter PEP-2 mediate CeTORC1 response to nutritional status. Current models set CeTORC1 as regulator of global mRNA translation, at least in part, by modulating S6K, PHA-4 and Box C/D snoRNPs. Autophagy is inhibited by active CeTORC1 signaling. Arrows represent activation and bars represent inhibition.

### *Downstream targets*

The mechanisms by which the TOR pathway controls growth and development in *C. elegans* are poorly understood.

CeTOR signals to the translation machinery and acts as a regulator of overall mRNA translation (54). Inhibiting translation by reducing the levels of ribosomal proteins or of *rsks-1/S6K* extends lifespan, and this effect has been found to mimic that of CeTOR inhibition (26). Although several translational regulators have been proposed as CeTOR targets (like eIF2 $\beta$ , eIF4E and eIF4G), their implication in CeTOR signaling is not clear yet (26, 86). In addition, CeTOR promotes the localization of box C/D snoRNPs to the nucleolus, which is required for rRNA maturation and robust protein synthesis (76). These observations support the hypothesis that CeTOR is a dominant upstream regulator of global translation in *C. elegans*, in contrast to its more limited role in mammals.

Recent studies revealed that CeTOR modulates the activity of the transcription factor *pha-4/FoxA*, a critical regulator of growth and longevity. *pha-4* is required for lifespan extension in response to diminished CeTOR signaling. What is more, inactivation of *rsks-1/S6K* suppressed the lethality associated with reduced *pha-4* activity. Together, CeTOR and S6K antagonize *pha-4* to control postembryonic development and longevity (76).

CeTOR is also involved in autophagy and prevention of necrotic cell death. Autophagy is essential for dauer morphogenesis and prevention of tissues aging in *C. elegans*. Consistent with the fact that inhibition of TOR activity induces autophagy in mammalian cells, reduced autophagy suppresses the long-lived phenotype of CeTOR mutant worms (25, 58, 91). Therefore, CeTOR signaling may affect dauer development and longevity by regulating autophagy.

## 2.4 Aim of this work

Evidence of mTOR signaling in the pathogenesis of polycystic kidney disease (PKD) has provided invaluable insight towards understanding cyst formation and disease progression. In the established mouse models many questions about proteins involved in PKD could be answered. However, the underlying events that regulate mTOR signaling remain poorly understood. Genetic studies in rodents are difficult to access and time consuming. Therefore, easy genetically tractable model organisms such as *C. elegans* are a promising mean to study the general *in vivo* principles of TOR functions.

The aim of this project was to establish the model organism *C. elegans* as a laboratory tool to study the TOR pathway *in vivo* and to gain insight into the genetic network of TOR signaling.

The first part of this study focused on basic functions of CeTOR and its transcriptional regulation. In order to define critical tissues and organs for CeTOR function, the expression pattern of CeTOR was analyzed. This was complemented by characterization of the phenotype resulting from RNAi-mediated gene knockdown of *CeTOR*.

The next purpose of this project was to set up an RNAi-based screening approach to identify novel components of the TOR signaling pathway. Therefore, a stable *let-363/CeTOR*-mutant strain was generated and a simple phenotypic assay was developed to screen for genetic interactors. With the herein established screening protocol large-scale setups will be manageable, so that systematic searches for genes affecting TOR function can be conducted by genome-wide RNAi analysis.

Finally, we used the *C. elegans* system in an attempt to reveal a genetic interaction between TOR and Hippo signaling, the two major pathways involved in cell growth and proliferation.

Since the fundamental mechanisms of TOR signaling are likely to be evolutionary conserved from nematodes to humans, this approach will help to better understand the operation of the TOR network.

## 3 Materials and methods

### 3.1 Materials

#### 3.1.1 Solutions and buffers

All solutions and buffers were prepared with ddH<sub>2</sub>O and were either autoclaved or sterile filtrated.

- 50x TAE ..... 242 g/l Trizma base  
57.1 ml/l Acetic acid, 100%  
18.6 g/l Na<sub>2</sub>EDTA 2xH<sub>2</sub>O
- 1x TAE ..... 60 ml 50x TAE  
200µl Ethidium bromide  
→ fill up to 3 l with ddH<sub>2</sub>O
- M9 buffer ..... 3 g/l KH<sub>2</sub>PO<sub>4</sub>  
6 g/l Na<sub>2</sub>HPO<sub>4</sub>  
5 g/l NaCl  
Optional 1 mM MgSO<sub>4</sub>
- 2x bleach solution ..... 0.5 M KOH  
2% NaOCl
- Worm lysis buffer ..... 10 mM Tris, pH 8.2  
50 mM KCl  
2.5 mM MgCl<sub>2</sub>  
0.45% NP40  
0.45% Tween 20  
0.01% Gelatine  
0.5 mg/ml Proteinase K
- Proteinase K ..... 10 mM Tris HCl, pH 7.5  
20 mM CaCl<sub>2</sub>  
50% Glycerol  
20 mg/ml proteinase K
- Worm freezing buffer ..... 100 mM NaCl  
50 mM KH<sub>2</sub>PO<sub>4</sub>, pH 6  
30% Glycerol  
1 M NaOH  
Optional 100 mM MgSO<sub>4</sub>

- 1M Potassium phosphate buffer, pH6.....108.53 g/l  $\text{KH}_2\text{PO}_4$   
46.22 g/l  $\text{K}_2\text{HPO}_4 \cdot 3\text{H}_2\text{O}$
- 1M Potassium citrate, pH6.....20 g/l Citric acid monohydrate  
293.5 g/l Tri-potassium citrate monohydrate
- S Basal.....5.85 g/l NaCl  
1 g/l  $\text{K}_2\text{HPO}_4$   
6 g/l  $\text{KH}_2\text{PO}_4$   
5 mg/l Cholesterol
- Trace metals solution.....1.86 g/l Disodium EDTA  
0.69 g/l  $\text{FeSO}_4 \cdot 7\text{H}_2\text{O}$   
0.2 g/l  $\text{MnCl}_2 \cdot 4\text{H}_2\text{O}$   
0.29 g/l  $\text{ZnSO}_4 \cdot 7\text{H}_2\text{O}$   
0.025 g/l  $\text{CuSO}_4 \cdot 5\text{H}_2\text{O}$

### 3.1.2 Media

- DYT.....16 g/l Bacto-trypton  
10 g/l Yeast-extract  
5 g/l NaCl
- Luria-Bertani (LB)-medium.....10 g/l Bacto-trypton  
5 g/l Yeast-extract  
5 g/l NaCl  
→ add 15 g/l agar for plates
- Ampicillin (in ddH<sub>2</sub>O).....100 µg/ml final concentration
- Tetracycline (in EtOH).....12.5 µg/ml final concentration
- Ampicillin/Tetracycline.....50 µg/ml-12.5 µg/ml final concentration
- NGM-Agar.....3 g/l NaCl  
17 g/l Agar  
2.5 g/l Bacto-peptone  
5 µg/ml Cholesterol  
1 mM  $\text{CaCl}_2$   
1 mM  $\text{MgSO}_4$   
25 ml/l 1M Potassium phosphate buffer, pH6  
20 µg/l Nystatin
- NGM-Agar for RNAi.....add 1mM IPTG  
add 100 µg/ml ampicillin

- S Medium ..... 1 l S Basal  
10 ml 1M Potassium citrate, pH6  
10 ml Trace metals solution  
3 ml 1M CaCl<sub>2</sub>  
3 ml 1M MgSO<sub>4</sub>

### 3.1.3 *C. elegans* strains

Table 1. *C. elegans* strains used in this study

Strain	Genotype	Name used
N2 Bristol	wild-type	wild-type
NL2099	<i>rrf-3(pk1426)</i>	<i>rrf-3</i>
DR2381	<i>let-363(h111)/dpy-5(e61)</i>	<i>let-363/dpy-5</i>
ENH92	<i>cst-1(tm1900)</i>	<i>cst-1</i>
ENH109	<i>Ex[let-363P1::gfp;rol-6(su1006)]</i>	<i>Ex[let-363P1::gfp]</i>
ENH112	<i>Ex[let-363P2::gfp;rol-6(su1006)]</i>	<i>Ex[let-363P2::gfp]</i>
ENH116	<i>Ex[let-363P3::gfp;rol-6(su1006)]</i>	<i>Ex[let-363P3::gfp]</i>
ENH122	<i>Ex[daf-15P::gfp;rol-6(su1006)]</i>	<i>Ex[daf-15P::gfp]</i>
ENH81	<i>let-363(h111); Ex[B0261;myo-2P::gfp]</i>	<i>let-363(h111);Ex[let-363;myo-2P::gfp]</i>
ENH108	<i>let-363(h111);rrf-3(pk1426);Ex[B0261;myo-2P::gfp]</i>	<i>let-363(h111);rrf-3(pk1426); Ex[let-363;myo-2P::gfp]</i>

### 3.1.4 Bacteria strains

Table 2. Bacteria strains used in this study.

Strain	Genotype
OP50 <i>E. coli</i>	<i>ura-</i>
HT115 (DE3) <i>E. coli</i>	F-, <i>mcrA</i> , <i>mcrB</i> , IN( <i>rrnD-rrnE</i> ) 1, <i>rnc14::Tn10</i> (DE3 lysogen: <i>lacUV5</i> promoter-T7 polymerase) (IPTG-inducible T7 polymerase) (RNase III minus) (Tetracycline resistance)
DH10B-T1 <i>E. coli</i>	F- <i>mcrA</i> Δ( <i>mrr-hsdRMS-mcrBC</i> ) φ80d <i>lacZ</i> ΔM15 <i>lacX74 recA1 endA1 araD139</i> Δ( <i>ara leu</i> )7697 <i>galJ galK rpsL nupG λ-tonA</i>



### 3.1.5 Plasmids and vectors

Table 3. Plasmids and vectors used in this study.

Name	Description	Resistance
pPD95.75	GFP-tagged vector for expression in <i>C. elegans</i> .	Amp
L4440 (pPD129.36)	RNAi vector, with two T7 promoters for production of dsRNA in HT115 <i>E. coli</i> .	Amp
B0261 Cosmid	Cosmid containing <i>let-363</i> and approximately 6.4 Kbp upstream of its start codon.	Amp
pRF4 ( <i>rol-6</i> )	<i>rol-6(su1006)</i> ; used as co-injection marker.	Amp
<i>myo-2P::eGFP</i>	<i>myo-2P::gfp</i> ; used as co-injection marker.	Kan
pBluescript II SK (+)	Bacterial expression vector; used to adjust the total DNA concentration of injection mixtures to 100 ng/μl.	Amp
<i>let-363P1::gfp</i>	5' region of <i>let-363</i> tagged with <i>gfp</i> . Cloned from B0261 cosmid into pPD95.75 with primers ENH181/ES64.	Amp
<i>let-363P2::gfp</i>	Operon promoter of <i>let-363</i> tagged with <i>gfp</i> . Cloned from B0261 cosmid into pPD95.75 with primers ENH182/ENH183.	Amp
<i>let-363P3::gfp</i>	Complete promoter of <i>let-363</i> tagged with <i>gfp</i> . Cloned from B0261 cosmid into pPD95.75 with primers ENH182/ES64.	Amp
<i>daf-15P::gfp</i>	<i>daf-15</i> promoter tagged with <i>gfp</i> . Cloned from wild-type mRNA (RT-PCR) into pPD95.75 with primers AT37/AT38.	Amp
pBY1933	<i>let-363</i> RNAi construct, from genomic DNA; results in a weak TOR phenotype.	Amp
pBY1934	<i>let-363</i> RNAi construct, from coding DNA; results in a strong TOR phenotype.	Amp
<i>cst-1</i> RNAi	<i>cst-1</i> RNAi construct. Cloned from cDNA library into L4440 with primers ES78/ES79.	Amp

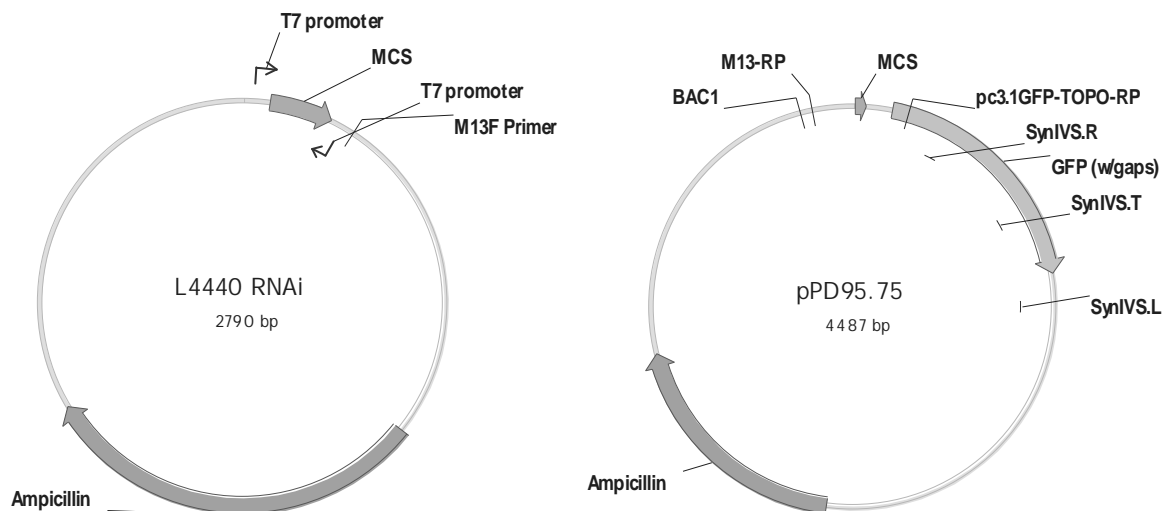


Figure 6. Maps of the vectors used in this study. L4440 (pPD129.36) was used to generate RNAi-expressing bacterial clones. pPD95.75 was used for GFP expression analyses in *C. elegans*. MCS: multiple cloning site.

## 6.3 Primers

Table 4. Primers used in this study.

Name	Sequenz 5'-3'	Use
ES75_rrf-3_F	ATGGTGCCACGAGCTGCGTA	genotyping of <i>rrf-3(pk1426)</i>
ES76_rrf-3_Rout	CGTCTCAGGAAAAGCGCATC	
ES77_rrf-3_Rin	CCATTCTGTGCACGTTTCCA	
ENH145_cst-1F	GACCATACATGCACTGTTGACG	genotyping of <i>cst-1(tm1900)</i>
ENH146_cst-1R	TGAGAGTATCGCGCAAAACTGC	
ENH192_let363_F	CGATAGACAGAACAAGCAGC	Amplification (ENH192-193) and sequencing (ENH194) of <i>let-363(h111)</i> mutation site for genotyping
ENH193_let363_R	GACAACGATCAACCAGCTCG	
ENH194_let363_seq	CAATCGAATAGTCTCCGCTC	
ES78_cst1RNAi_F	CGGGATCCGGCGAAGGATCATATGGAAGC	cloning of <i>cst-1</i> RNAi
ES79_cst1RNAi_R	CGGGATCCACGCGCGGTGAGTTGCCATTTT	
ES64_let-363P_R	CGCGGATCCGCTGCATCTCTATTTTCCGTAATTG	cloning of <i>let-363</i> promoter constructs P1 and P3
ENH181_Sph_let363P_F1	CATGCATGCCAAGAGAGGAGCTCCACGAGTT	cloning of <i>let-363</i> promoter construct P1
ENH182_Sph_let363P_F2	CATGCATGCGATGTTGCTCTTGGCATTCTTGTGTTG	cloning of <i>let-363</i> promoter constructs P2 and P3
ENH183_BamH_let363P_R2	CGCGGATCCGCATATATAAGAGCAAAATATTCA	cloning of <i>let-363</i> promoter construct P2
AT37	GGTCTGCCCGGGTAAATCTGATTATATGATCAAG	cloning of <i>daf-15P::gfp</i>
AT38	CAACGCACGCGTCCGGCGGCCGCTCTGGTACCTTTG	
ENH184_let363_RT	GCATCTCTATTTTCCGTAATTG	RT-PCR and 5' RACE PCR of <i>let-363</i>
SL1	GGTTTAATTACCCAAGTTTGAG	
SL2	GGTTTTAACCCAGTTACTCAAG	
M13-FP (GATC)	TGTAACGACGCGCCAGT	sequencing of constructs cloned in L4440 vector
pc3.1GFP-Topo-RP (GATC)	CCCATTAAACATCACC	sequencing of constructs cloned in pPD95.75 vector

## 3.2 Molecular biology methods

### 3.2.1 Polymerase chain reaction (PCR)

PCR is used to amplify DNA fragments by *in vitro* enzymatic reaction. As the PCR progresses, the DNA generated is used as a template for replication, producing an exponential amplification and generating millions of copies of the DNA piece.

There are diverse DNA polymerases available, each one of them needing different reaction conditions and components (see manufacturer's instructions).

PCR was used to amplify DNA fragments with specific restriction sites for cloning, to test the orientation and ligation success rate of single clones (colony-PCR), and to determine the genotype of individual worms (single worm PCR).

### **3.2.2 RNA isolation from *C. elegans* and reverse transcriptase PCR (RT-PCR)**

The RT-PCR is used to amplify a defined fragment of an RNA molecule. The RNA strand is first reverse-transcribed into its complementary DNA, followed by amplification of the resulting DNA using PCR.

For *C. elegans* RNA isolation, wild-type worms from a not starved plate were several times washed with M9 Buffer (with MgSO<sub>4</sub>) and rapidly frozen in liquid nitrogen. The frozen worm pellet was then homogenized in a sterile mortar with a pestle, keeping it always in liquid nitrogen, and RNA isolation and purification was carried out using the RNeasy<sup>®</sup> Mini Kit.

The second step, converting RNA to DNA, was carried out using the Superscript III Reverse Transcriptase according to the manufacturer's protocol and a gene specific primer. After the reverse transcriptase reaction was completed, the generated DNA from the original single stranded mRNA was used as template in a standard PCR with Taq polymerase.

RT-PCR was used in this study for the analysis of the 5' region of *let-363* transcript.

### **3.2.3 Cloning procedure**

With the cloning process DNA fragments are inserted in vectors (bacterial plasmids) to be expressed in *C. elegans*, cells or bacteria. Here is described a standard cloning procedure:

The DNA fragment of interest was amplified by PCR using oligonucleotides with specific recognition sites for restriction enzymes. The proofreading polymerases OptiTaq or KOD were used for DNA amplification. The amplified DNA and the vector were cut with the appropriate restriction endonucleases at the optimal temperature and conditions according to the manufacturer.

Ligation of vector and insert was performed with T4 ligase. DNA fragment and vector were mixed in a ratio 5:1 and the ligation mixture was incubated at least two hours at 25°C or overnight at 15°C.

Bacteria transformation is the genetic alteration resulting from the uptake of foreign DNA. The ability of these cells to take up exogenous DNA from the environment is called competence. The ligation mixture was used for transformation in chemically competent DH10 *E. coli* cells. 50 µl of bacterial suspension and 5 µl of ligation reaction were incubated for 20 minutes on ice. After a 50 seconds heat shock at 42°C, the DH10 *E. coli* cells were streaked on LB-agar plates containing the appropriate antibiotic and incubated overnight at 37°C.

To identify positive clones, either single colony-PCR or restriction digestion of previously isolated plasmids was performed. For the colony-PCR, individual bacteria colonies were picked with a sterile pipette tip, incubated one hour at 37°C in LB-medium and added to a PCR reaction mixture with specific oligonucleotides and Taq polymerase. For the isolation of plasmids, the QIAprep® Spin Miniprep Kit or the NucleoBond® Xtra Maxi Kit were used.

Plasmids were sequenced by GATC Biotech AG, Konstanz, Germany.

### **3.3 *C. elegans* methods**

#### **3.3.1 Breeding of *C. elegans***

##### *Culturing C.elegans on petri plates*

*C. elegans* is usually maintained in the laboratory on Nematode Growth Medium (NGM) agar plates seeded with the *E. coli* strain OP50, and kept in air permeable cardboard boxes at 15, 20 or 23°C (10, 51, 83).

Several methods are used for transferring *C. elegans* from one petri plate to another. The method mainly used in this study was to pick single animals with a worm picker, which was made by mounting a piece of platinum wire into the tip of a Pasteur pipet. Platinum wire heats and cools quickly and can be flamed between transfers to avoid contamination. The end of the wire, used for picking up worms, was flattened slightly. To transfer worms from a starved plate, a sterilized scalpel was used to move a chunk of agar to a fresh plate (“chunking”).

The frequency of transferring the worms depends on their genotype, the selected breeding temperature and the experiment. In general, stocks were kept at 15°C and experiments took place at 20°C.

For decontamination of *C. elegans* strains, a drop of sodium hypochlorite and sodium hydroxide 1:1 mixture was placed on the edge of a plate and adult worms were then added. The solution kills contaminants and worms, but does not destroy the eggs, which are resistant and survive.

#### *Growth of C. elegans in liquid medium*

Liquid cultures of *C. elegans* are usually grown in S medium using concentrated OP50 *E. coli* as a food source. OP50 *E. coli* pellets were kept at -20°C in 45 ml falcon tubes and S medium was added and mixed with the bacteria.

#### *Freezing of C. elegans*

*C. elegans* can be frozen and stored for years at -80°C or indefinitely in liquid nitrogen (-196°C). Only L1-L2 larvae survive the freezing process.

For every strain to be frozen a large NGM plate (Ø 9 cm) with lots of freshly starved L1-L2 animals was washed several times with M9 buffer (with MgSO<sub>4</sub>). After the final washing step, the worm pellet was resuspended in M9 buffer and one volume of freezing buffer was added. Finally, the worms were transferred to cryovials and gradually cooled down.

Thawing was made at room temperature. The content was then poured onto a large NGM plate seeded with OP50 *E. coli*.

### **3.3.2 Synchronization of *C. elegans* strains**

In order to have staged worms, adult animals were washed off from an NGM plate (Ø 9 cm). One volume of bleach solution was added and the mixture was vigorously shaken for 5-10 minutes to isolate the hypochlorite-resistant eggs. After several washing steps, the pellet was resuspended in M9 buffer and incubated overnight on a rotation mixer at 15°C. Newly hatched L1 larvae in M9 buffer cannot evolve to the

next developmental stages because of food deprivation. The L1 larvae were finally centrifuged and transferred to NGM plates ( $\varnothing$  9 cm) seeded with OP50 *E. coli*.

An alternative staging method used consisted in placing adult worms on NGM plates seeded with OP50 *E. coli* and allowing them to lay eggs for approximately five hours. After that, the adult worms were removed from the plate and the eggs let to develop at 15 or 20°C.

For small scale synchronization of *C. elegans* strains, a drop of sodium hypochlorite and sodium hydroxide 1:1 mixture was first placed on the edge of a plate. Adult worms were then added. The solution kills the worms but not the eggs, and soaks into the plate before the embryos hatch.

### **3.3.3 Genotyping of *C. elegans* by single worm PCR**

Single worms were transferred into individual PCR tubes using a pipette with 2  $\mu$ l worm lysis buffer and frozen at -80°C for at least 40 minutes. This was followed by incubation at 65°C for one hour, which resulted in lysis of the worm and release of the genomic DNA. Proteinase K was inactivated by incubation at 95°C for five minutes. The worm lysate was then used as template for PCR with primers designed to distinguish between wild-type and mutant alleles by producing two DNA fragments different in size.

### **3.3.4 Microinjection of *C. elegans***

Microinjection is an effective method for DNA transformation in *C. elegans* used frequently for the creation of transgenic strains. The DNA is directly injected into the worm's gonad, which contains a central core of syncytial germ cells. This approach usually leads to the formation of large extrachromosomal DNA arrays containing hundreds of copies of the co-injected plasmids that can be delivered to the progeny.

The DNA was introduced into the animals using the gonad injection method described by C. Mello and A. Fire (59). In some cases the plasmids were linearized prior microinjection, since this has been reported to increase the expression rate in *C. elegans*. The injection mix contained a selectable marker to facilitate the identification of transformants in the progeny. For the purposes of this study, *myo-2P::gfp* (staining the pharynx with the fluorescent marker GFP) or *rol-6* (resulting in a

roller phenotype) were used as co-injection markers. Animals of the first progeny generation expressing the co-injection marker were singled. Individuals transferring the marker to the second generation were considered to be an extrachromosomal transgenic line.

Table 5. *C. elegans* transgenic strains generated in this study.

Strain	Genotype	Injected plasmid	Co-injection marker	Injected strain	Name used
ENH109	<i>Ex[let-363P1::gfp/rol-6(su1006)]</i>	linearized <i>let-363P1::gfp</i> 10 ng/μl	pRF4 ( <i>rol-6</i> ) 40 ng/μl	wild-type	<i>Ex[let-363 P1::gfp]</i>
ENH112	<i>Ex[let-363P2::gfp/rol-6(su1006)]</i>	linearized <i>let-363P2::gfp</i> 10 ng/μl	pRF4 ( <i>rol-6</i> ) 40 ng/μl	wild-type	<i>Ex[let-363 P2::gfp]</i>
ENH116	<i>Ex[let-363P3::gfp/rol-6(su1006)]</i>	linearized <i>let-363P3::gfp</i> 10 ng/μl	pRF4 ( <i>rol-6</i> ) 40 ng/μl	wild-type	<i>Ex[let-363 P3::gfp]</i>
ENH122	<i>Ex[daf-15P::gfp/rol-6(su1006)]</i>	<i>daf-15P::gfp</i> 10 ng/μl	pRF4 ( <i>rol-6</i> ) 40 ng/μl	wild-type	<i>Ex[daf-15P::gfp]</i>
ENH81	<i>let-363(h111); Ex[B0261;myo-2P::gfp]</i>	B0261 Cosmid 25 ng/μl	<i>myo-2P::eGFP</i> 20 ng/μl	<i>let-363/dpy-5</i>	<i>let-363(h111); Ex[let-363;myo-2P::gfp]</i>

### 3.3.5 Crossing of *C. elegans* strains

#### *Genetic crosses*

Although *C. elegans* hermaphrodites usually reproduce by self-fertilization, they are also able to mate with males, and then cross-fertilization takes place. In the laboratory, crossing *C. elegans* hermaphrodites with males can be manipulated to transfer genetic material and produce progeny with desired genotypes.

As a standard, L4 hermaphrodites were placed with males at a ratio of 1:5 on small NGM plates (Ø 3.5 cm) at 15°C for mating. After 24h, the hermaphrodites were transferred to individual fresh plates (P generation). The success of the crosses was monitored by the amount of males in the F1 generation, where the ratio of hermaphrodites to males should be approximately 1:1. About 8-10 hermaphrodites of the F1 generation were singled and their progeny was further analyzed. The corresponding mutations in the F2 generation were identified either by single worm PCR, visual markers (GFP) or morphological phenotypes, and confirmed in the following generations. The strain *let-363(h111);rrf-3(pk1426);Ex[let-363;myo-2P::gfp]* was generated using this method (Fig. 6) (see chapter 4.2.2).

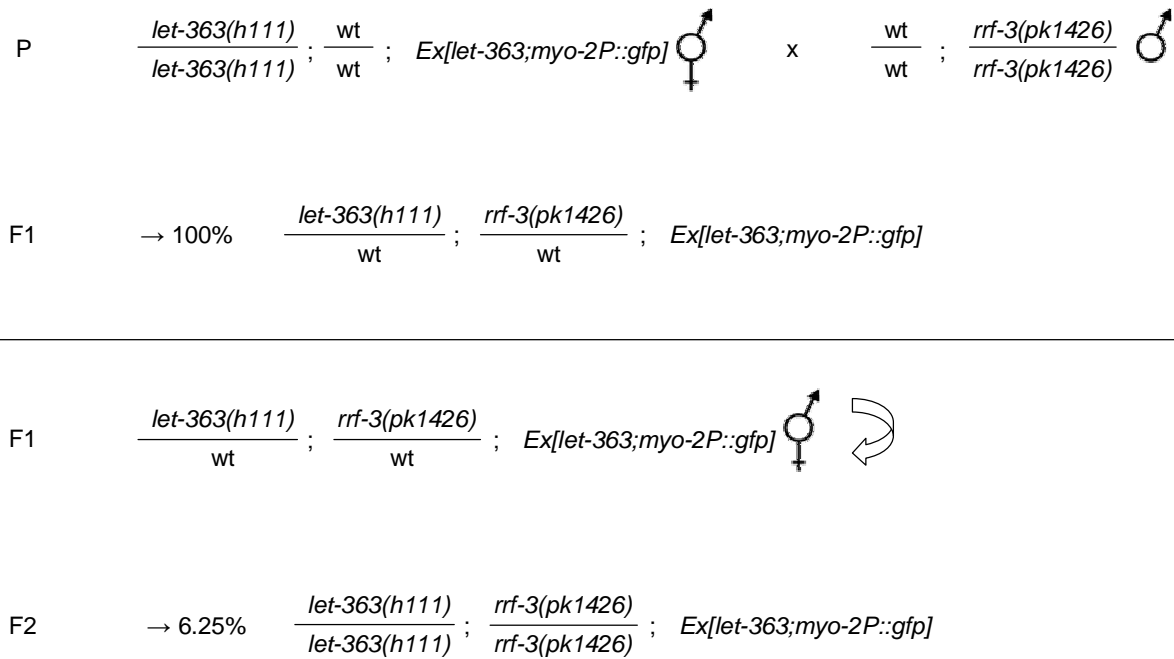


Figure 7. Crossing schema used to generate the strain *let-363(h111);rrf-3(pk1426);Ex[let-363;myo-2P::gfp]*. In every step, only worms carrying the GFP marker, that is, the extrachromosomal array containing wild-type *let-363*, were selected. *let-363(h111);Ex[let-363;myo-2P::gfp]* hermaphrodites were crossed with *rrf-3(pk1426)* mutant males. 100% of the cross-fertilized progeny was heterozygote for both mutations. Hermaphrodites of the F1 generation were allowed produce self-fertilized progeny. 6.25% of the F2 generation was expected to be homozygote for both mutations. To detect the *rrf-3* mutation, analysis of genomic DNA was performed by single worm PCR after allowing singled worms to produce progeny by self-fertilization. Only the F3 generation descending from *rrf-3* homozygotes was further analyzed in search of *let-363* mutation. The worms were first selected by their phenotype, that is, transgenic adults and not transgenic L3-arrested larvae. Afterwards, to confirm the *let-363* mutation, the region containing the point mutation was amplified by PCR and the product was sent for sequencing. The C/T substitution (wild-type/mutant) was confirmed in five different PCR reactions of five different worms lacking the transgenic marker from two different generations. *rrf-3* genotyping PCR was repeated three times with 10-15 worms each time on the next generations to confirm the presence of an homozygous *rrf-3* mutation.

### Outcrossing

All mutant strains generated have to be crossed at least 3 times with *C. elegans* wild-type animals prior analysis. Outcrossing is essential for the elimination of possible mutations in other genes that could interfere with the desired mutant phenotype. For this reason, the mutant strain *cst-1(tm1900)* was crossed 3 times with wild-type worms (Fig. 7) (see chapter 4.3.3)



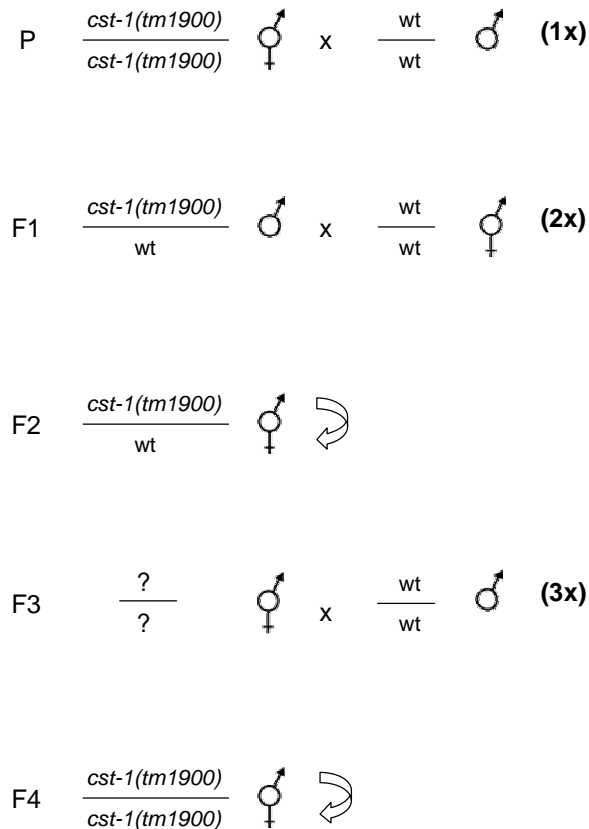


Figure 8. Outcrossing schema of *cst-1(tm1900)*. In the first crossing step (1x), *cst-1* hermaphrodites were crossed with wild-type males, and males of the F1 generation of crossed-progeny were used for the second cross with wild-type hermaphrodites (2x). The mutated *cst-1(tm1900)* allele was detected on the F2 generation by single worm PCR after allowing singled worms to produce progeny by self-fertilization. F3-generation hermaphrodites descending from *cst-1* heterozygotes, which could be *cst-1* homozygote, *cst-1* heterozygote or wild-type, were crossed with wild-type males in the final crossing step (3x), allowed to lay eggs on individual plates and finally genotyped by single worm PCR. On the F4 generation, only hermaphrodites descending from *cst-1* homozygotes were selected and their progeny further analyzed. Genotyping was repeated three times on the following generations to confirm the homozygosis of the *cst-1(tm1900)* mutant strain

### 3.3.6 RNA interference (RNAi)

RNA interference (RNAi) is a method for post-transcriptional targeted gene silencing. The introduction of double stranded RNA (dsRNA) into cells or tissues triggers degradation of the cognate mRNA. In *C. elegans*, dsRNA can be delivered efficiently by several methods, like injecting or soaking the animals with *in vitro* transcribed dsRNA or, more simply, feeding the animals bacteria expressing dsRNA that is homologous to the target gene (20, 89).

## RNAi feeding

The gene of interest was cloned into vector L4440 (containing an ampicillin-resistance gene) flanked by two T7 RNA polymerase promoters, and then transformed into the *E. coli* strain HT115 (DE3) (Fig. 9). These bacteria harbour an IPTG-inducible T7 RNA polymerase within an integrated Tn10 transposon that confers tetracycline resistance. When exposed to IPTG, the bacteria express the T7 RNA polymerase, which results in production of dsRNA homologous to the DNA inserted between the T7 promoter sites. When worms eat these bacteria, they release dsRNA, which is absorbed through the gut where it acts to silence gene expression. In a poorly understood process, this silencing effect rapidly spreads throughout the organism to silence gene expression in other tissues.

To prepare the bacteria, single colonies of bacterial clones containing the desired RNAi plasmids were allowed to grow overnight in LB-Amp/Tet. The preparatory cultures were used to inoculate the main cultures 1:50 in LB-Amp, and these allowed to grow for eight hours at 37°C before seeding the plates. The production of dsRNA was induced by adding 1 mM IPTG to NMG-RNAi agar plates. This induction was best achieved when seeding the plates with a very thin lawn of bacteria 1 day after pouring them. NGM-RNAi plates also contained ampicillin for a better bacteria selection. Plates with HT115 containing the empty L4440 vector were simultaneously prepared and used as control.

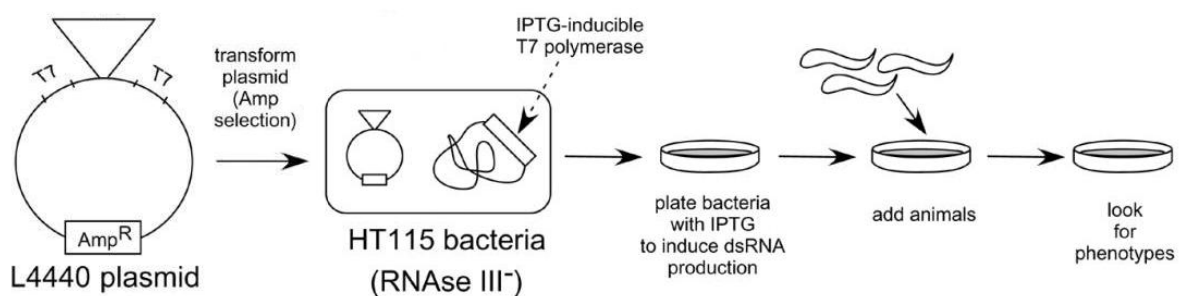


Figure 9. Schematic representation of RNAi by feeding bacteria expressing dsRNA to *C. elegans*. The ampicillin-resistant plasmid L4440 contains gene-specific DNA flanked by two T7 RNA polymerase binding sites. It is transformed into HT115 bacteria, which contain an IPTG-inducible T7 polymerase that facilitates the production of dsRNA. When exposed to IPTG, HT115 bacteria express the T7 polymerase and produce dsRNA. Feeding the worms dsRNA-expressing bacteria releases the dsRNA and induces silencing of the targeted gene. Source: Ann K. Corsi (14); modified.

## Working with RNAi

The *C. elegans* strain *rrf-3(pk1426)* is one of various strains hypersensitive to RNAi. *rrf-3* encodes a putative RNA-directed RNA polymerase that inhibits somatic RNAi, and its loss-of-function mutation results in enhanced sensitivity to RNAi (80). *rrf-3* mutant worms were used for analyses of RNAi phenotypes and to test the intensity of the IPTG induction before working with this or other mutant strains, for example, prior to a lifespan assay.

### 3.3.7 RNAi screening

This RNAi screening protocol has been designed taking as a starting point those described by J. Ahringer and B. Lehner (2, 48), adapting the method to the aims of our study. Its liquid format allows the performance of thousands of parallel experiments, making possible the fast completion of the entire genome within weeks. The experiments were carried out in 96-well plates, each well containing one RNAi clone from the *C. elegans* RNAi feeding library grown in liquid culture. *let-363(h111);rrf-3(pk1426)* mutants (from the strain *let-363(h111);rrf-3(pk1426);Ex[let-363;myo-2P::gfp]*) were exposed to dsRNA-expressing bacteria from the L1 larval stage, and the phenotype of the F1 generation scored for suppression of the *let-363* arrest phenotype (see chapter 4.3.3). As control, the whole procedure was performed in parallel with *rrf-3(pk1426)* mutants.

**1. Preparation of bacteria and worms:** Performing a genome-wide RNAi screen requires the coordination of bacterial and worm cultures. This entails several preparatory steps that have to be performed in parallel during two days before starting the experiment:

- Preparation of bacteria: bacterial cultures were inoculated from a glycerol stock to a flat bottomed 96-well plate, containing each well 50  $\mu$ l LB-medium with tetracyclin (12,5  $\mu$ g/ml) and carbenicillin (50  $\mu$ g/ml). Carbenicillin belongs to the same antibiotic group as ampicillin, and provides stronger bacterial selection. Cultures were let to grow overnight at 28°C with shaking. On the second day, IPTG was added to the cultures to a final concentration of 1mM to induce the production of dsRNA. Bacteria were further incubated for 1-2h at 28°C to ensure robust dsRNA induction.

- Preparation of worms: worms were synchronized following the standard bleaching procedure described in 3.3.2, which entails leaving the eggs at 15°C to hatch overnight. On the next day, newly hatched L1 larvae were resuspended in S-Basal (containing standard S-Basal additives plus 1mM IPTG and 50 µg/ml carbenicillin) at a concentration of approximately 30 worms per 20 µl.

2. *RNAi feeding*: a 20 µl aliquot of worm solution was pipetted into each well of the plates containing one bacterial clone after IPTG induction took place. Finally, the plates were placed at 20°C with shaking for aeration.

3. *Scoring of phenotypes*: plates were scored after 72 and 96 hours. By this point, bacteria had been partially consumed and worms could be easily analyzed under a dissection microscope. Plates were re-scored on days 7-8 to analyze the phenotype of the F1 generation.

### 3.3.8 Larval arrest test

This test was designed to perform *let-363* epistasis experiments. For this purpose, the L3-arrest phenotype of *let-363*-deficient worms treated with RNAi was used as read-out.

The mutant strain *rrf-3(pk1426)* was selected to perform this test, since the strong RNAi phenotype exhibited facilitates the recognition of the different stages. However, arrested *rrf-3*-mutant *let-363*-deficient larvae are small and difficult to see in the bacteria. Therefore, the number of arrested worms was indirectly calculated by comparing the number of eggs laid with the number of not arrested worms found three days later.

L4 *rrf-3*-mutant larvae were transferred to the desired RNAi plates and kept at 20°C. Approximately 24 hours later, the worms were allowed to lay eggs on new plates, and the eggs laid were scored. After three days at 20°C, when the staged worms on control plates had reached adulthood, every plate was inspected and the worms classified in two groups: arrested L3 and not arrested adults. The gonads of animals in an intermediate stage were examined, and only those producing eggs were included in the not arrested group.

### 3.3.9 Determination of *C. elegans* lifespan

For the determination of *C. elegans* lifespan in RNAi experiments, worms were first synchronized by allowing adult worms to lay eggs for four to six hours on control plates. All steps of the lifespan assay took place at 20°C.

100-150 young adult worms were transferred to RNAi plates. This was considered day 0 of the experiment. The worms were transferred to fresh plates every day until progeny production ceased, and every five days afterwards, until all worms died. The number of worms alive was determined every day, and dead worms were removed from the plate. Worms were considered dead when no touch-provoked movement was observed. Wild-type worms on RNAi and control plates were used as control.

Animals that crawled off the plate, exhibited extruded internal organs or displayed an Egl phenotype, that is, egg laying defective with the subsequent hatching of larvae inside the mother, were censored.

All lifespan assays were repeated at least three times. SigmaStat 3.5 software (STATCON) was used to calculate mean adult life span and to perform statistical analysis. *P*-values were determined using a log-rank test (Mantel-Cox).

#### 3.3.10 Microscopy

For expression studies, animals were mounted on 2% agarose in M9 buffer pads containing 5-10 mM sodium azide, and examined by fluorescence microscopy as described by J. E. Sulston and H. R Horvitz (85). Images were taken with 20x and 40x objectives on a Zeiss Axioplan2 microscope, with an AxioCam camera and the AxioVision software Rel.4.7, using an EGFP filter set (480/20-nm excitation, 510/20-nm emission).

## 4. Results

### 4.1 Analysis of *let-363/CeTOR* expression in *C. elegans*

#### 4.1.1 *let-363/CeTOR* is *trans*-spliced and locates in an operon

During the formation of mature mRNA, introns are removed from the pre-mRNA and exons are spliced together in a precisely regulated manner. This process, which is common to all eukaryotes, is called *cis*-splicing. In nematodes, however, there is an additional process for transcript maturation called *trans*-splicing, in which a 22 nucleotide RNA sequence, the spliced leader (SL), is spliced on to the 5' end of the pre-mRNA. There are two *trans*-spliced leaders: SL1, which is the most commonly used, and SL2. Approximately 70% of all *C. elegans* genes are *trans*-spliced (7, 9).

Another interesting characteristic of *C. elegans* is that a considerable part of its genome (about 15%) is organized in operons. An operon is a cluster of identically oriented closely-spaced genes that are co-expressed under the control of a single promoter. Genes residing in operons are transcribed into one polycistronic pre-mRNA, and then processed by *trans*-splicing to generate monocistronic mRNAs, which are latterly translated individually. SL2 *trans*-splicing occurs exclusively in genes that are located downstream in an operon. The SL2 *trans*-spliced leader is never found in genes that are monocistronic or genes situated most upstream of an operon. However, a combination of both SL1 and SL2 *trans*-splicing is possible for genes residing downstream in an operon (7, 9).

*C. elegans* TOR homologue (CeTOR) is encoded by *let-363*, which is predicted to be located in an operon together with B0261.4, a gene that encodes a mitochondrial ribosomal protein (Fig. 10A). The small distance between both genes, of only 488 bp, suggests that *let-363/CeTOR* may be transcribed downstream of B0261.4 in a polycistronic pre-mRNA and afterwards *trans*-spliced in an SL2 manner. To test this hypothesis, the 5' region of *let-363* was analyzed by RT-PCR to determine which spliced leader *let-363* receives. RT-PCR was performed from wild-type worms with a *let-363* gene-specific reverse primer (complementary to nucleotides 224 to 246 of *let-363*) and an upstream oligonucleotide equivalent to the SL1 or SL2 sequence. As shown in figure 10B, a strong product of approximately 250 bp was detected with the SL2 primer, indicating that *let-363* pre-mRNA is SL2 *trans*-spliced. Although a faint

SL1 product was also detected, the observation that most *let-363* mRNA begins with SL2 indicates that *let-363* is primarily expressed in an operon. Alternatively, *let-363* might have two promoters: one upstream of B0261.4 that results in co-transcription of *let-363* and B0261.4, from which the SL2-spliced gene product is generated, and a second promoter close to the 5' end of *let-363*, from which the SL1-spliced mRNA is generated.

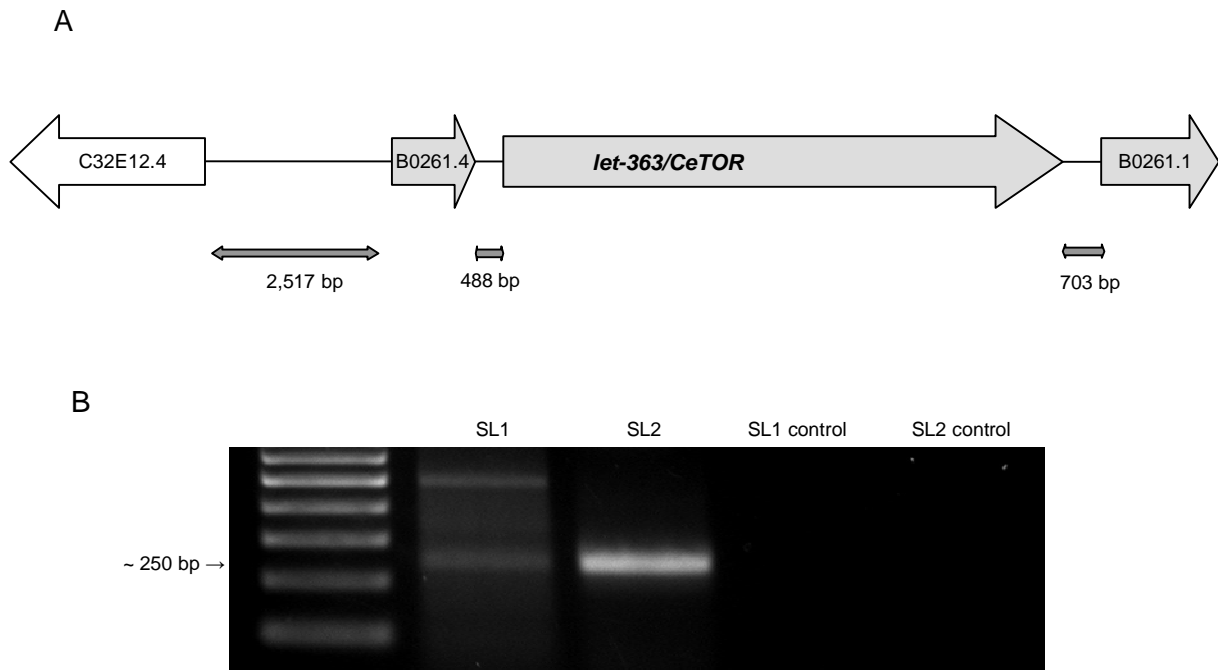


Figure 10. *let-363/CeTOR* is *trans*-spliced and locates in an operon. **A** Schematic representation of genomic *let-363/CeTOR*, the genes situated upstream of it, and the closest downstream gene. B0261.4 and *let-363/CeTOR* are separated by 488 bp, and *let-363/CeTOR* and B0261.1 by 703 bp. Therefore, the three genes are predicted to be part of the same operon. **B** RT-PCR made with RNA from wild-type worms, performed with a *let-363* gene-specific reverse primer (ENH184) and an SL1 or SL2 specific primer. Controls lacking template showed no signal.

#### 4.1.2 Analysis of *let-363/CeTOR* transcriptional regulation and expression pattern

Using RT-PCR we could show that *let-363/CeTOR* is, at least partially, SL2 *trans*-spliced and resides in an operon. Consequently, *let-363* and B0261.4 are supposed to be transcribed under the control of a common regulatory signal situated upstream of B0261.4. To study the transcriptional regulation of *let-363* and determine its expression pattern, three different genomic sequences of the predicted *let-363* promoter were fused with GFP (Fig. 11). The construct *let-363P1::gfp* (P1) contains the genomic sequence between B0261.4 and *let-363* together with the first 248 bp of *let-363*, including its first exon and intron and part of its second exon. We assumed that this region contains an internal promoter inside the operon situated directly next to *let-363*. The second construct, *let-363P2::gfp* (P2), contains the sequence between B0261.4 transcription initiation site and its closest upstream gene partner, C32E12.4. This region was assumed to represent the core promoter of the operon. The third construct, *let-363P3::gfp* (P3), carries the complete predicted promoter: the sequence enclosed between C32E12.4 and *let-363*, including B0261.4. These GFP-reporter constructs were then used to generate transgenic lines by microinjection into wild-type animals (Tab. 5). As *C. elegans* is transparent throughout its entire life, the GFP-reporter gene expression can be easily visualized. Several transgenic lines were analyzed to exclude mosaicism and loss of expression.

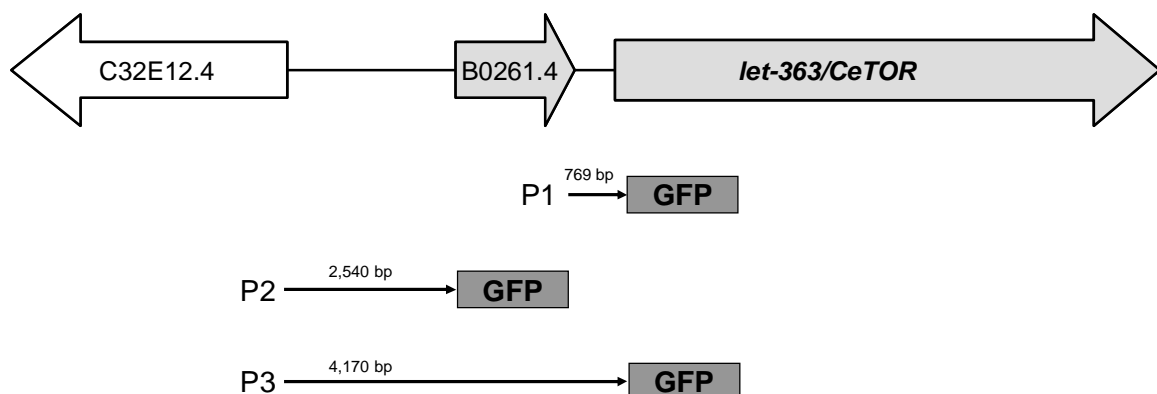


Figure 11. Schema of *let-363/CeTOR* promoter constructs. Three different genomic regions of the predicted *let-363* promoter were cloned into a GFP tagged vector (pPD95.75). P1: 769 bp; intergenic region between B0261.4 and *let-363*. P2: 2,540 bp; intergenic region between C32E12.4 and B0261.4. P3: 4,170 bp; sequence between C32E12.4 and *let-363*.



### *Expression pattern of let-363P1::gfp*

The promoter construct *let-363P1::gfp* was expressed during all developmental stages, and could be first detected during embryonic development (Fig. 12A). The strongest GFP expression was observed in recently hatched L1, and then it gradually decreased during all post-embryonic stages until adulthood. GFP staining was observed in head and tail neurons, all segments of the pharynx and intestinal cells (Fig. 12B-E). Interestingly, *let-363P1::gfp* expression was particularly strong in the ASI neurons, situated in the head, which are involved in chemotaxis and control the entry into dauer stage (4). Cells situated at the beginning and end of the intestinal tract exhibited higher fluorescence intensity than the rest of the intestine, in which some cells seemed to display no fluorescence at all. This observation might indicate that the reporter construct P1 lacks important control elements for stable intestinal expression. Furthermore, it has been reported that *let-363* is ubiquitously expressed in *C. elegans* (54). Since *let-262P1::gfp* is not expressed in all tissues, we assume that the intergenic region between *let-363* and B0261.4 does not contain the entire *let-363* promoter.

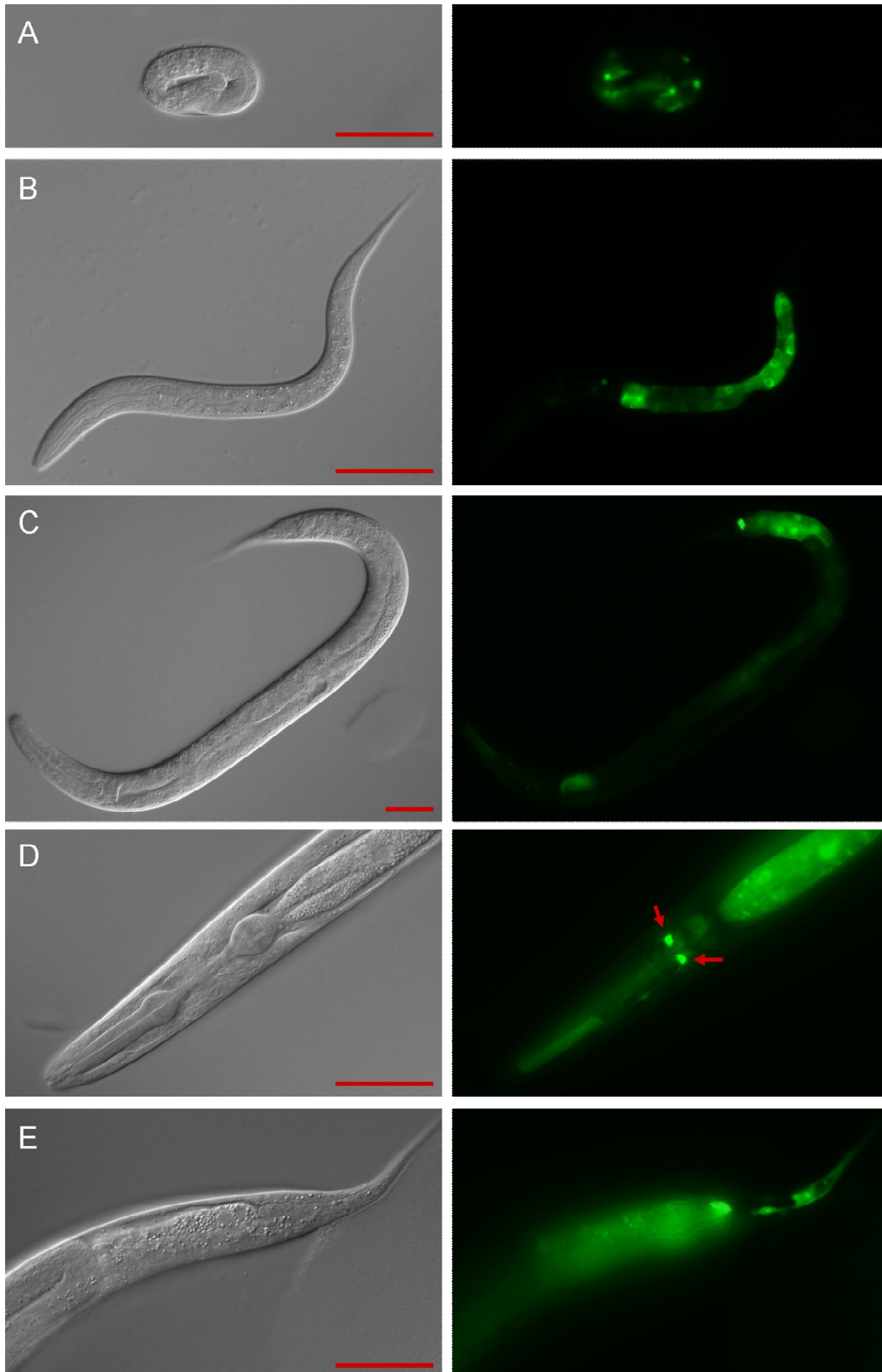


Figure 12. Expression pattern of *let-363P1::gfp*. Pictures on the left are DIC micrographs of *Ex[let-363P1::gfp]* worms; the corresponding fluorescence pictures (GFP) are shown on the right. **A** Expression in a 3-fold embryo. **B** Expression in L1 larval stage. **C** Expression in L3 larval stage. **D** Head region of an L4 larva. Arrows point to the ASI neurons. **E** Tail region of an L4 larva. Images were taken with 20x and 40x objectives using an EGFP filter. Scale bars represent 50  $\mu$ m.

### *Expression pattern of let-363P2::gfp*

Expression of *let-363P2::gfp* resulted in a constant pattern in all larval stages and adulthood. Weak GFP staining was detected in the pharynx, the vulva, the spermatheca and tail neurons (Fig. 13). The fluorescence pattern observed in the intestinal cells most likely corresponded to auto-fluorescence. In all 3 independent transgenic lines examined, the fluorescence intensity was very weak, but whether this was due to incomplete expression of the array or the result of the transcriptional regulation of this reporter construct could not be distinguished. Therefore, a more detailed examination could not be performed.

Expression of the *let-363*-GFP reporter driven by the genomic region contained in the P2 construct did not result in a stable and ubiquitous pattern. However, it included expression in tissues not stained by *let-363P1::gfp*, such as the vulva and the spermatheca, indicating that both segments are not sufficient but necessary for total expression of *let-363*.

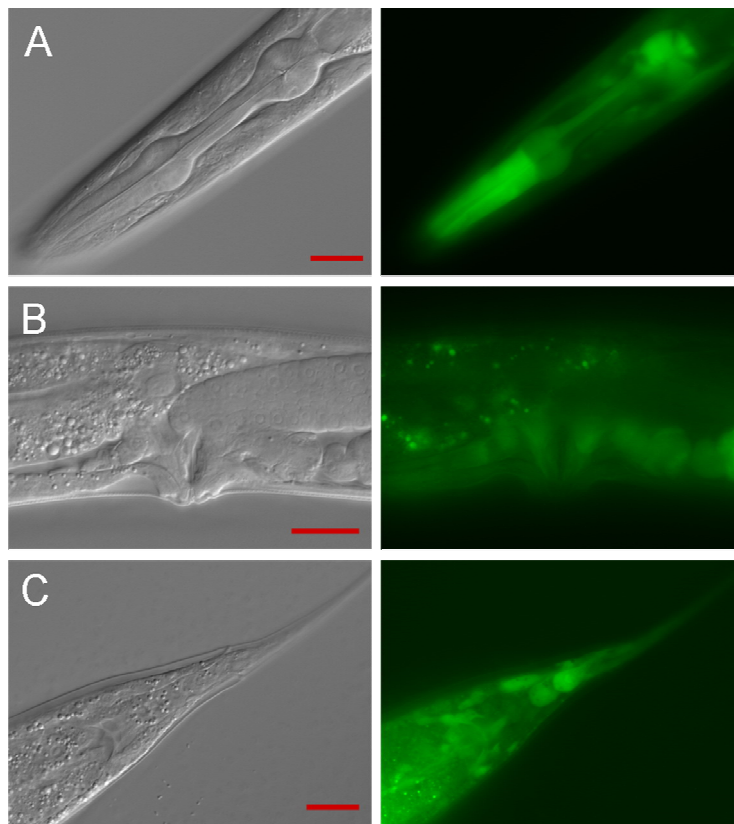


Figure 13. Expression of *let-363P2::gfp* in an L4 larva. On the left: DIC pictures; on the right: corresponding GFP micrographs. **A** Head region. **B** Vulva and spermatheca. **C** Tail region. Images were taken with a 40x objective using an EGFP filter. Scale bar represents 20  $\mu\text{m}$ .

### *Expression pattern of let-363P3::gfp*

*let-363P3::gfp* was ubiquitously expressed, and fluorescence was observed in all studied tissues throughout all developmental stages, including embryonic development. GFP staining was strongly observed in head and tail neurons, all segments of the pharynx, intestine, vulva, spermatheca, distal tip cells, somatic muscle and hypodermis (Fig. 14).

This 4,170 bp promoter construct, which includes 3,922 bp upstream of *let-363* start codon and the first 248 bp of *let-363*, was expressed in tissues that were not stained by the reporter constructs P1 and P2. This expression pattern of *let-363P3::gfp* corresponds to that described in previous reports, showing ubiquitous expression of *let-363* driven by 7 Kbp upstream regulatory sequence (54).

Taken together, we assumed that the complete promoter of *let-363/CeTOR* encloses the whole 3.9 Kbp upstream region of *let-363*, including B0261.4. Within this sequence, there might be complex and distant control elements which are needed to ensure proper and robust *let-363* expression.

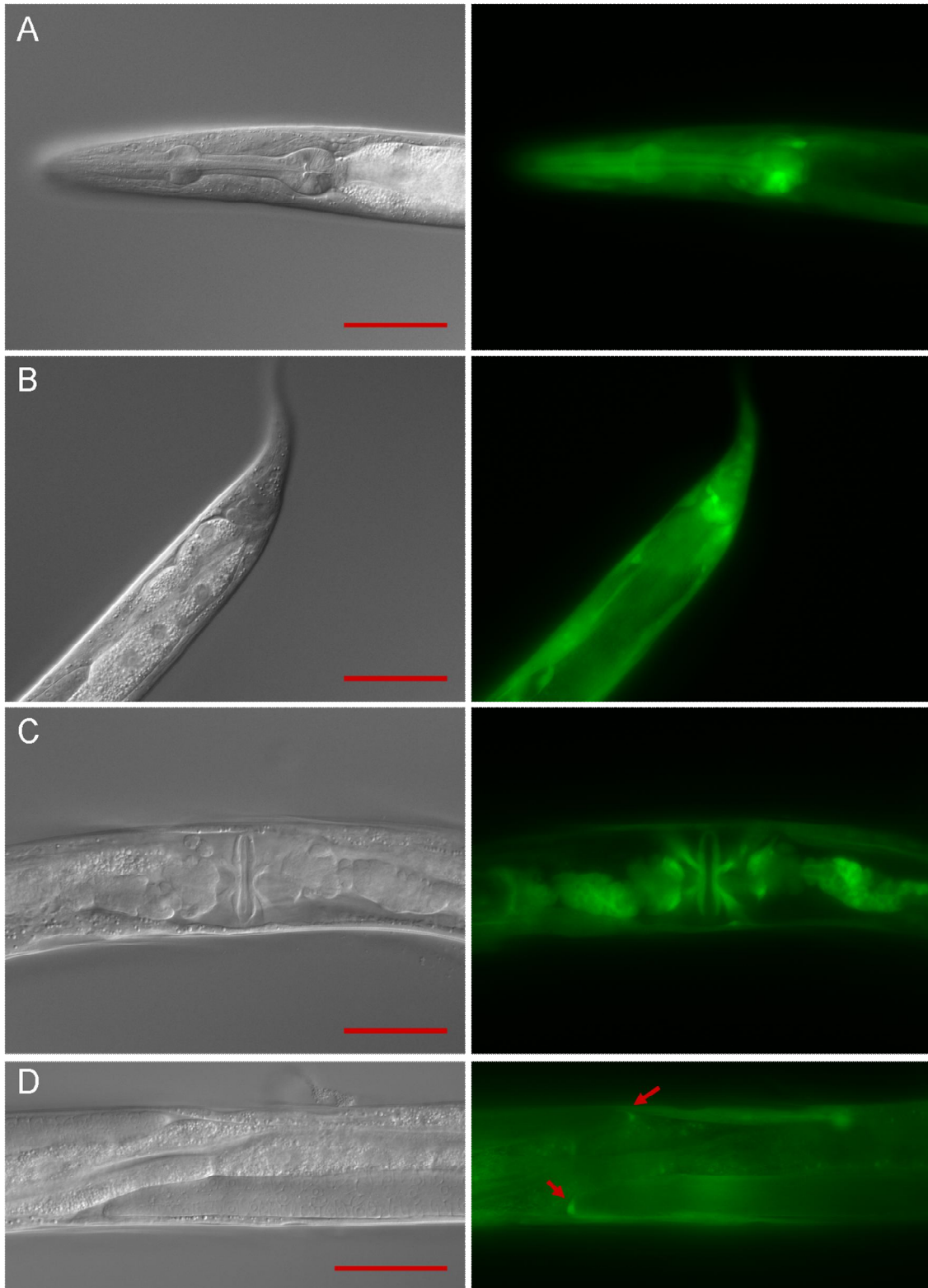


Figure 14. Expression pattern of *let-363P3::gfp*. The DIC micrographs shown are of *Ex[let-363P3::gfp]* L4 larvae and were taken with a 40x objective; their corresponding fluorescence pictures were made using an EGFP filter. **A** Head region. **B** Tail region. **C** Vulvar muscles and spermatheca. **D** Intestine and gonads. Arrows point to the distal tip cells. Scale bar represents 50  $\mu\text{m}$ .

### 4.1.3 The expression pattern of *daf-15/CeRaptor* resembles that of *let-363/CeTOR*

DAF-15 is the *C. elegans* homologue of mammalian Raptor, and it is believed to interact with CeTOR to form the TOR complex 1 in *C. elegans* (37). Given the predicted interaction between *daf-15/CeRaptor* and *let-363/CeTOR*, a similar expression pattern should be expected. To analyze the expression pattern of *daf-15*, a transcriptional reporter containing 1.8 Kbp of upstream regulatory sequence fused with GFP was cloned and transformed into *C. elegans* wild-type worms by microinjection (Tab. 5).

GFP staining was observed in most tissues throughout all developmental stages. This included head and tail neurons, all segments of the pharynx, intestine, vulva, distal tip cells, somatic muscle and hypodermis, showing that *daf-15* is ubiquitously expressed (Fig. 15). This pattern largely overlaps the expression pattern of *let-363*, supporting the hypothesis of both proteins acting together as a complex.

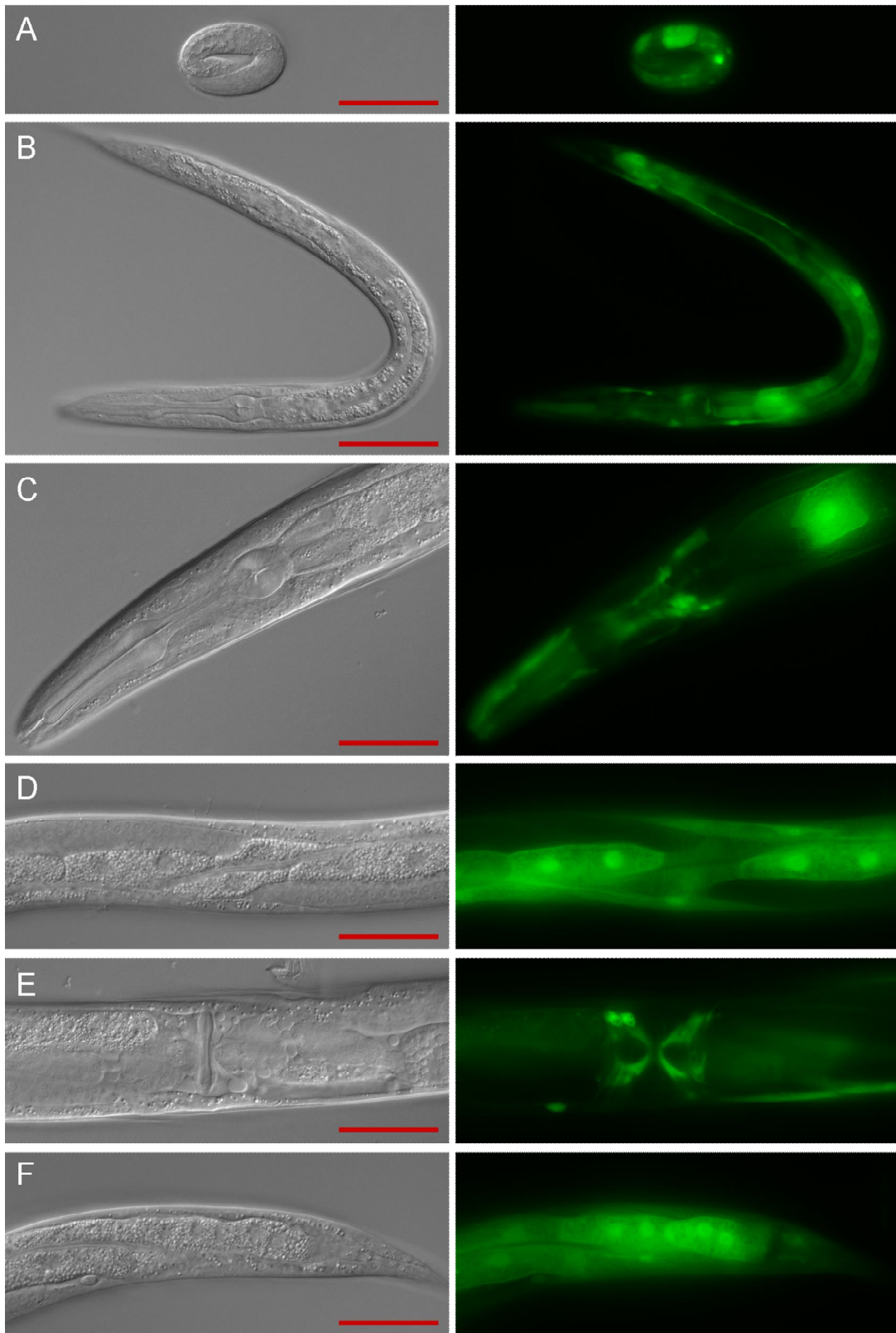


Figure 15. Expression pattern of *daf-15P::gfp*. Pictures on the left are DIC micrographs; the corresponding GFP are shown on the right. **A** Expression in a 3-fold embryo. **B** L2 larva. **C** Head region of an L4 larva. **D** Intestine and gonad of an L4 larva. **E** Vulvar muscles of an L4 larva. **F** Tail region of an L4 larva. Images were taken with a 40x objective using an EGFP filter. Scale bar represents 50  $\mu$ m.

## 4.2 Knockdown of *let-363/CeTOR* in *C. elegans* results in a pleiotropic phenotype

In this study we attempted to use the *C. elegans* system in search for novel modulators of the TOR signaling pathway. For this purpose, we needed to start by characterizing *let-363/CeTOR* knockdown phenotype.

TOR signaling regulates larval development, metabolism and aging in *C. elegans* (54). Under normal growth conditions, *C. elegans* undergoes four larval molts and reaches reproductive adulthood within three days. However, homozygous *let-363/CeTOR* mutants irreversibly arrest development at the L3 larval stage (Fig. 16A-B) (54). Since *let-363/CeTOR* null mutants show developmental arrest and are in turn lethal, we first evaluated the effect of partial loss of TOR function on larval development and lifespan.

Gene knockdown can be efficiently achieved by dsRNA-mediated interference (RNAi). Thereby, worms are fed bacteria producing dsRNA homologous to a predicted gene, which triggers the degradation of the corresponding mRNA (20). To induce a partial knockdown of *let-363/CeTOR*, *let-363*RNAi by feeding was established. The phenotypic effect of feeding RNAi can vary depending on the genetic background and the developmental stage of the worms. Thus, different RNAi feeding conditions were analyzed. We tested the effect of feeding *let-363*RNAi on development using the mutant strain *rrf-3(pk1426)*. *rrf-3* encodes a putative RNA-directed RNA polymerase that inhibits somatic RNAi. Mutation of *rrf-3* results in hypersensitivity to RNAi, which provides an optimal background for a more effective RNAi-mediated gene silencing (80). Two different *let-363*RNAi constructs were tested: pBY1934 and pBY1933. pBY1934 produces dsRNA that is homologous to coding *let-363*, while pBY1933 produces dsRNA complementary to genomic *let-363*. When *rrf-3(pk1426)* mutants were exposed to the *let-363*RNAi construct pBY1934 starting from the L4 larval stage, they developed into apparently normal adults. However, almost 100% of their F1 generation arrested at the L3 larval stage, displaying a CeTOR-deficient phenotype resembling that of homozygous *let-363(h111)* mutants. Exposing *rrf-3(pk1426)* L4 larvae to bacteria generating *let-363*RNAi from pBY1933 had a weaker and heterogeneous effect on the F1 generation, producing L3 arrest at variable proportions ranging from 30 to 70% (Fig. 16C). Worms overcoming developmental arrest were usually smaller than wild-type



and displayed an undefined phenotype between L4-stage and adulthood. However, despite an apparent gonadal immaturity, some of them were able to produce progeny. As feeding pBY1934 starting from the L4 stage displayed the strongest and most stable effect, we used these conditions in further genetic experiments.

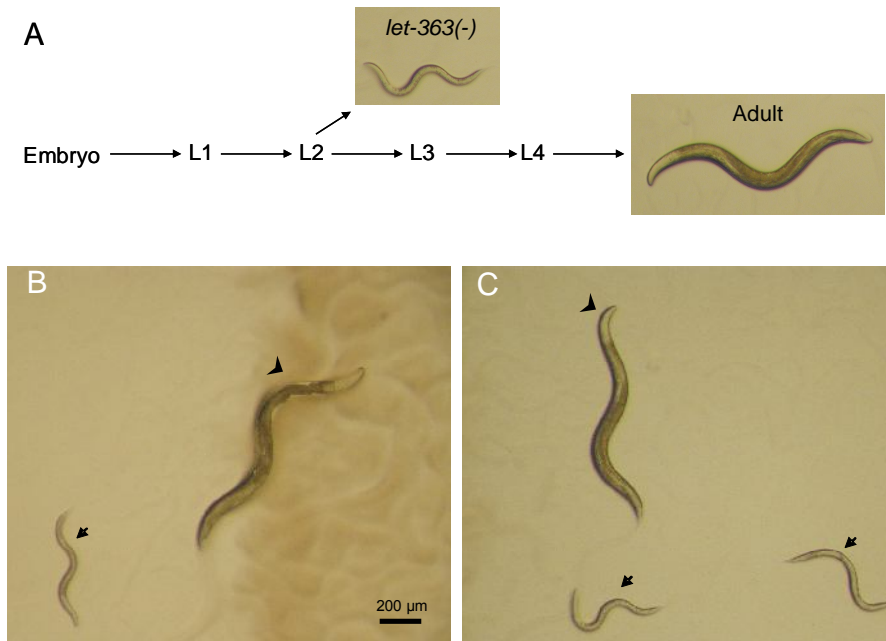


Figure 16. CeTOR-knockdown by RNAi resembles the phenotype of *let-363/CeTOR* mutation. **A** *let-363*-deficient worms arrest development at the L3 larval stage and are not able to complete their life cycle and reach adulthood. **B** Homozygous *let-363(h111)* arrested larva (arrow) from the balanced mutant strain *let-363(h111)/dpy-5(e61)*, next to a wild-type-like *let-363/dpy* heterozygote (arrowhead). **C** *rrf-3(pk1426)* worms exposed to *let-363*RNAi by feeding (pBY1933): L3 arrested larvae (arrows) next to an *rrf-3* adult (arrowhead). Photos were taken under a dissection microscope.

We evaluated another possible way of blocking CeTOR signaling: treating the worms with rapamycin. In yeast and mammals, rapamycin is a potent and selective inhibitor of TORC1. It is not clear how rapamycin acts, but it is believed that, in complex with FKBP12, it can provoke the disassociation of TOR and Raptor, and therefore disrupt TORC1 function (98). To test the effect of rapamycin in *C. elegans*, we injected different concentrations of rapamycin ranging from 10 nM to 500 nM into the gonad or the intestine of L4 larvae and adult worms, and analyzed their progeny. Here we could not observe the developmental arrest phenotype of CeTOR deficient worms, as rapamycin treated animals normally developed to adults. Neither microinjection nor treatment with rapamycin by feeding seemed to have an effect in the worms or their progeny. The same happened when soaking the animals in liquid culture containing

rapamycin in concentrations from 100 nM to 10  $\mu$ M (data not shown). Rapamycin is poorly soluble in water; thus, it was dissolved in DMSO for its administration. For this reason, higher concentrations of rapamycin could not be tested, since the solvent DMSO per se was toxic for the worms. Therefore, we could not distinguish between a natural resistance of *C. elegans* against rapamycin or an insufficient drug concentration inside the animals.

Homozygous *let-363*-mutant worms exhibit many other features apart from arresting development at the L3 larval stage. In addition, these larvae display an extended mean lifespan of 25 days at 25.5°C compared to 10 days in wild-type animals (93). However, it is difficult to analyze the effect of CeTOR on lifespan comparing different developmental stages (arrested larvae versus adult worms). Therefore, we tested the effect of knocking down CeTOR after the L3 stage with RNAi. Wild-type worms were fed with *let-363*RNAi (pBY1934) starting from the first day of adulthood. The mean lifespan of worms on *let-363*RNAi was  $19.6 \pm 0.4$  days at 20°C compared to  $14.6 \pm 0.3$  days for wild-type worms fed with control RNAi (Fig 17). Furthermore, animals treated with *let-363*RNAi exhibited a delay on the upcoming of age-related signs, like reduction of body movement or decrease in rate of the pharyngeal pumping. Together, knockdown of CeTOR after the L3 stage results in a more discreet but still extended lifespan, which indicates that this phenotypical feature is CeTOR-dependent, and not a consequence of the developmental arrest.

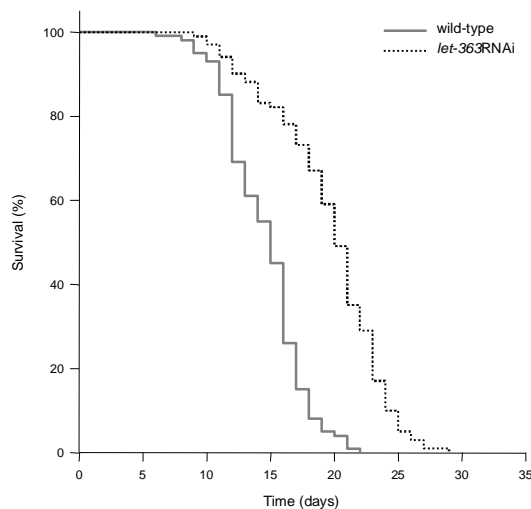


Figure 17. Knockout of CeTOR by feeding *let-363*RNAi from the first day of adulthood extends lifespan. Wild-type mean lifespan=  $14.6 \pm 0.3$  days ( $n=125$ ); *let-363*RNAi mean lifespan=  $19.6 \pm 0.4$  days ( $n=126$ );  $P$ -value  $< 0.001$ . Data presented as: mean lifespan (days)  $\pm$  standard error of the mean;  $n$  represents number of animals observed.

### 4.3 Genome-wide RNAi screening for genes that modulate CeTOR function

The discovery of RNA interference (RNAi) in *C. elegans* allows the rapid silencing of gene activity in order to access its underlying function. Gene knockdown can be easily achieved by feeding bacteria expressing dsRNA, which triggers the degradation of the homologous mRNA. An RNAi bacterial feeding library has been assembled, covering 86% of the *C. elegans* predicted genes (21, 40). Recent research has shown that large-scale experimental setups using this library are manageable, so that systematic analyses of gene functions and genetic pathways can be conducted (21, 41, 66, 79).

Here we developed a strategy for systematic searches for genes affecting CeTOR function by genome-wide RNAi analysis. Therefore, all relevant techniques necessary for using *C. elegans* as a model organism, including generation of transgenic *let-363* mutant animals, RNAi technology, and RNAi-screening, were established.

#### 4.3.1 Generation of a stable *let-363/CeTOR* mutant strain for RNAi screening approaches

Homozygous mutation of *let-363/CeTOR* is lethal, since arrest of larval development blocks reproduction. To stably keep *let-363* strains carrying recessive lethal mutations, the worms have to be maintained as heterozygotes. However, in heterozygous strains the mutation can be lost easily through segregation unless there is a morphological marker to identify it. Therefore, the *let-363* mutation was linked to a visible marker *in trans*: in the mutant strain *let-363(h111)/dpy-5(e61)* (kindly provided by D. Riddle), *dpy-5* has been introduced close to the wild-type allele of *let-363* as genetic balancer, and *in trans* to the lethal *let-363* mutation. This way, homozygous *dpy-5* (which are wild-type for *let-363*) can be easily recognised by their short and fat bodies (dumpy phenotype) while heterozygotes can be identified by their wild-type phenotype. Together, self-progeny of *let-363(h111)/dpy-5(e61)* are either L3-arrested *let-363* homozygotes, wild-type-like *let-363/dpy-5* heterozygotes, or dumpy *dpy-5* homozygotes (Fig. 18).

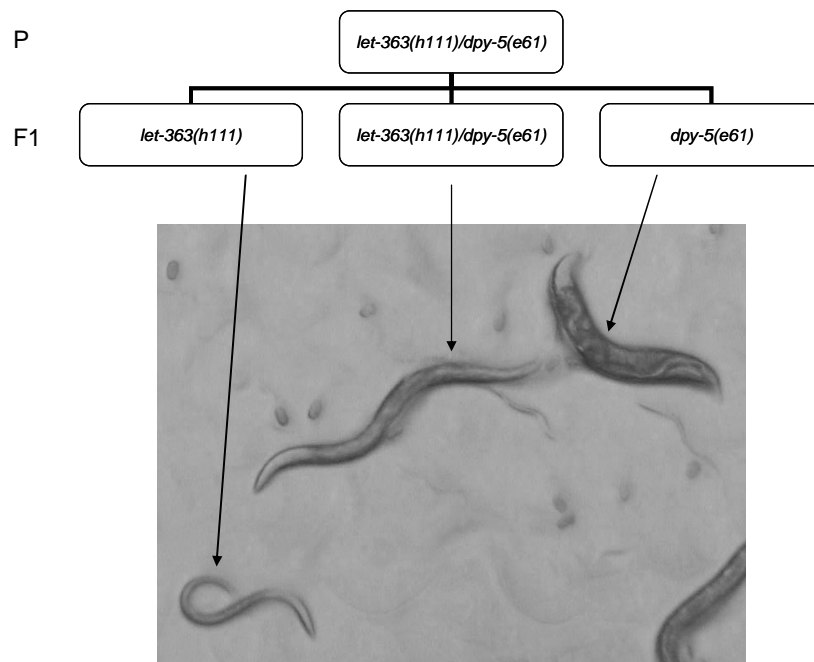


Figure 18. Segregation and phenotype of *let-363(h111)/dpy-5(e61)* mutant strain. The self-progeny of *let-363(h111)/dpy-5(e61)* is constituted by 25% *let-363(h111)* homozygotes (arrested L3 larvae), 25% *dpy-5(e61)* homozygotes (dumpy phenotype), and 50% heterozygotes (wild-type phenotype).

In our RNAi screening approach, we propose to screen for suppression of the L3-arrest phenotype of homozygous *let-363* mutants. Since in our RNAi screen not-arrested *let-363* homozygotes would not be phenotypically distinguishable from *let-363/dpy-5* heterozygotes, we could not use this strain. Therefore, we generated a new *let-363* homozygous mutant strain replacing the *dpy-5* balancer with a GFP-marked balancer, allowing phenotypical differentiation.

We introduced the CeTOR cosmid B0261 as extra-chromosomal balancer in *let-363* mutants. The cosmid B0261 contains the entire *let-363/CeTOR* wild-type coding sequence and control elements, and expression of wild-type *let-363* from this cosmid was expected to complement and rescue the mutant phenotype. Transformation of *let-363* mutants was performed by microinjection of the CeTOR cosmid into heterozygous *let-363(h111)/dpy-5(e65)* (Tab. 5). The CeTOR cosmid was injected together with *myo-2P::gfp* as co-injection marker. Microinjected DNA molecules assemble into a large array containing hundreds of copies of co-injected plasmids (59), in this case wild-type *let-363* and *myo-2P::gfp*. Expression of *myo-2P::gfp* stains the pharynx with the fluorescent marker GFP, facilitating the recognition of transformants. Individual transgenic worms expressing the fluorescent marker were

transferred to new plates and their progeny was examined for loss of *dpy-5*. Only those plates where the worms had lost the *dpy*-balancer and no trace of the dumpy phenotype was observed were selected, that is, homozygous for *let-363*. The strain was referred as *let-363(h111);Ex[let-363;myo-2P::gfp]*. Three independent lines were generated, finding no significant differences between them.

Expression of *let-363* from the cosmid was able to complement the *let-363* mutant phenotype, and thus, allowed homozygotes to develop into adults capable of producing progeny. The transgenic array was maintained extrachromosomally and transmitted to the progeny with a variable inheritance, which means that part of the progeny did not receive the array. Therefore, only worms expressing *myo-2P::gfp* carried the extrachromosomal array containing *let-363*, thus, producing the subsequent rescue effect. Consequently, *let-363* mutants that did not inherit the extrachromosomal rescue array (as marked by loss of GFP-staining) arrested at the L3 larval stage. Together, the progeny of transgenic *let-363(h111);Ex[let-363;myo-2P::gfp]* segregates in wild-type-like animals exhibiting the GFP marker and non-transgenic L3-arrested larvae (Fig. 19).

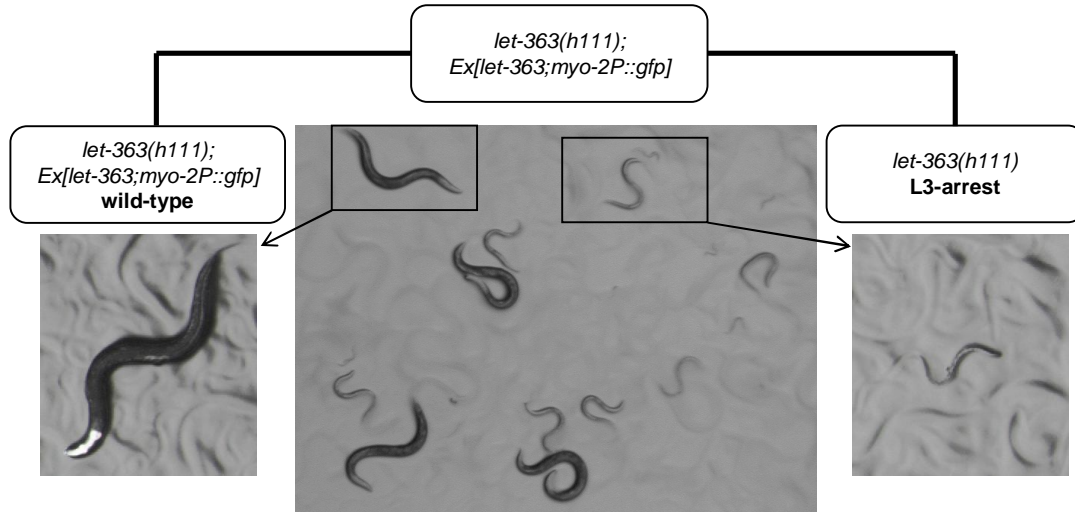


Figure 19. Balancing of *let-363* mutants by an extrachromosomal wild-type *let-363/CeTOR* array. Progeny of transgenic *let-363(h111);Ex[let-363;myo-2P::gfp]* segregates in wild-type-like and L3-arrested worms (photo in the middle). Fluorescence analysis confirms that only animals expressing the GFP marker, and therefore wild-type *CeTOR*, reach adulthood (on the left). Absence of GFP indicates loss of the wild-type *let-363/CeTOR* array, and thus homozygous *let-363* mutants arrest at the L3 stage (on the right). All animals were staged and kept at the same temperature to ensure synchronized growth.

Finally, for RNAi screening approaches, the strain *let-363(h111);Ex[let-363;myo-2P::gfp]* was crossed with *rrf-3(pk1426)*. Mutation in *rrf-3* results in hypersensitivity to RNAi (80), providing an optimal background for a more effective RNAi screening. This is especially important for genes involved in neuronal function, as neurons are much more resistant to RNAi than other cells. The crossing procedure and schema are described in chapter 3.3.5, figure 7. The strain was referred as *let-363(h111);rrf-3(pk1426);Ex[let-363;myo-2P::gfp]*.

#### **4.3.2 Design of a genome-wide RNAi screen for genes interacting with CeTOR to regulate larval development**

In this project we sought to identify modulators of CeTOR function and, therefore, we developed a strategy for a genome-wide feeding-based RNAi screen. As readout for our screen we chose the modulation of the developmental arrest at the L3 larval stage of *let-363/CeTOR* mutants. This L3-arrest is a very striking phenotype and modifications can be quickly monitored and scored by observing the worms under a dissection microscope.

By RNAi-mediated gene knockdown, we tested whether the block of larval development in *let-363* mutants can be released, allowing progression to adulthood. Therefore, *let-363* mutants balanced by a transgenic wild-type *let-363* array containing a GFP marker (described in more detail in chapter 4.3.1) were fed with individual RNAi-expressing bacterial clones from the Ahringer library (40). This RNAi feeding library contains approximately 16,700 bacterial strains, representing about 86% of the predicted *C. elegans* genome. The library is supplied in 96 well plates, each well containing a single bacterial clone producing dsRNA targeting one *C. elegans* gene.

For this study we established an RNAi-feeding protocol in liquid culture and adapted the conditions to our worm strains (described in more detail in materials and methods, chapter 3.3.7). In brief, *let-363(h111);rrf-3(pk1426)* mutants balanced with the transgenic array *Ex[let-363;myo-2P::gfp]* were fed with individual RNAi clones. We started with a synchronized worm population at the L1 stage and after 72 and 96 hours at 20°C the animals were screened for complete or partial suppression of the L3-arrest phenotype. After another 72-96 hours their progeny was also scored. *let-363;rrf-3* mutant worms that have lost the balancer array (also recognizable by loss of

the fluorescent GFP marker) arrest at the L3 larval stage, and we would expect that RNAi-mediated knockdown of a functional related gene can release the developmental block. Here one has to distinguish between adult worms where RNAi induces suppression of the *let-363* phenotype and those bearing the wild-type array reaching adulthood (Fig. 20). Together, suppression of the *let-363* mutant phenotype would be indicated by the presence of not-arrested worms lacking the GFP marker. Feeding RNAi clones to *rrf-3(pk1426)* mutants served as a control. This way, we expect to identify known genes in the TOR pathway (positive control) and novel related factors.

In a pilot screen we tested this protocol using the first 48 clones from the *C. elegans* RNAi feeding library. We did not observe suppression of the TOR mutant phenotype among these candidates. However, the completion of the whole genome-wide screen will surely provide us new hints in the search of CeTOR interactors. Recent technical advances may help to accomplish this challenging task, like the Complex Object Parametric Analyzer and Sorter, better known as COPAS Biosorter. This device can sort individual worms on the basis of length, optical density and fluorescence at rates up to 100 worms per second (68). Using the COPAS Biosorter might be highly useful for phenotype scoring, facilitating rapid separation of transgenic from non-transgenic worms by their fluorescence, and arrested from non-arrested mutants by their size.

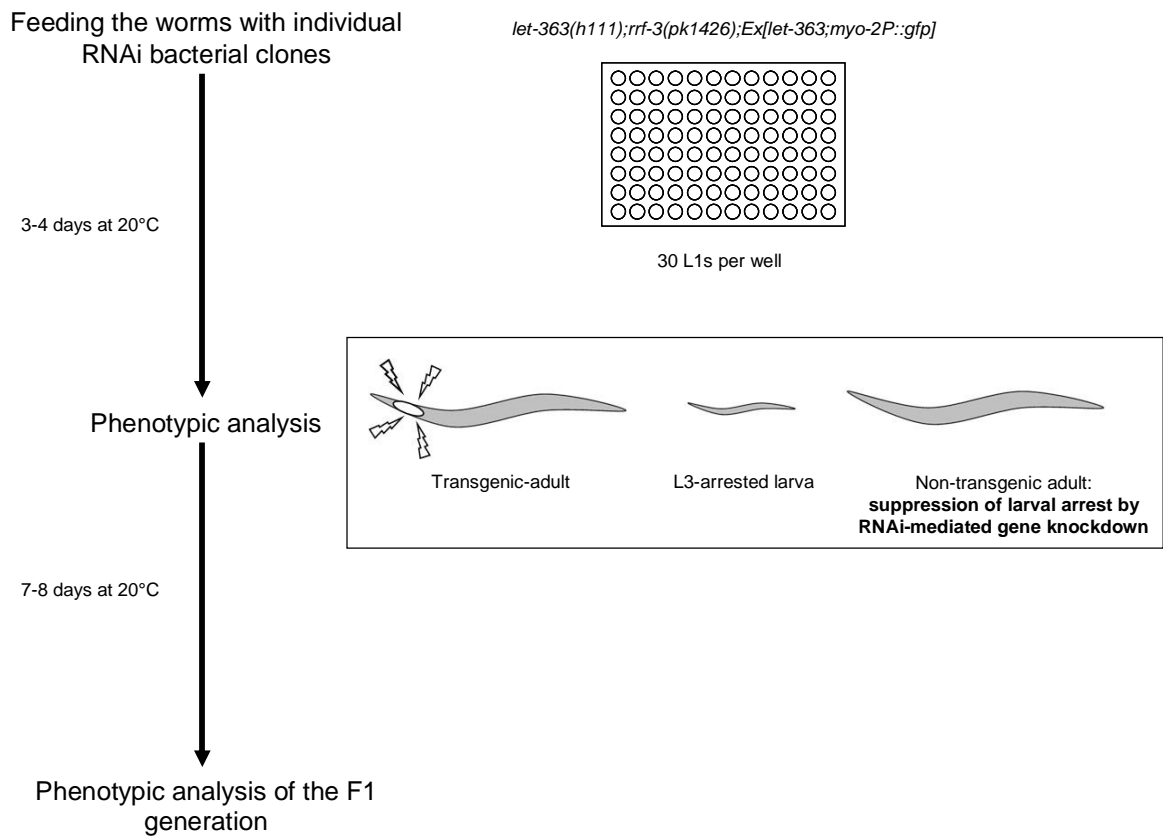


Figure 20. Schematic representation of an RNAi screening approach in liquid culture. Experiments are performed in 96-well plates where each well contains one individual bacterial clone expressing RNAi against one specific gene. *let-363(h111);rrf-3(pk1426)* mutants balanced with a transgenic *let-363* GFP-marked array are fed individual RNAi clones from the L1 stage. Animals are scored after 3-4 days at 20°C, and their F1 generation after 7-8 days. *let-363* mutants arrest development at the L3 larval stage, and only animals bearing the transgenic balancer (exhibiting the GFP marker) reach adulthood. Therefore, suppression of developmental arrest would be indicated by the presence of non-transgenic adults (lacking the GFP marker).



#### **4.4 Identification of a new CeTOR regulator: *MST1 C. elegans* orthologue *cst-1* modulates *let-363/CeTOR***

Insulin/IGF signaling is one of the most important pathways involved in the regulation of stress response and lifespan (5). In *C. elegans*, as in higher vertebrates, insulin/IGF antagonizes the FOXO transcription factors. In the worm, insulin/IGF-mediated inactivation of the FOXO transcription factor DAF-16 involves AKT/SGK-dependent phosphorylation and subsequent cytoplasmic retention. In conditions of reduced Insulin/IGF signaling, as well as under heat or oxidative stress, the inhibition of DAF-16 is released. Thereby, DAF-16 translocates to the nucleus and modulates genes required for stress response and longevity (30, 47, 52, 64).

An additional input into FOXO/DAF-16 is conferred by Mammalian Sterile Twenty kinases (MST), central components of the MST pathway (Hippo in *Drosophila*). The MST/Hippo pathway is highly conserved in evolution and has been implicated in a variety of biological functions, including cell proliferation, apoptosis, and response to environmental stress (75). In mammalian neurons, MST1 mediates oxidative stress-induced cell death by directly activating FOXO transcription factors. Furthermore, knockout of *cst-1/MST1* in *C. elegans* accelerates aging, while overexpression of *cst-1* induces lifespan extension in a *daf-16*-dependent manner (49). Together, these results indicate evolutionary conserved signaling links between MST1/CST-1 and the FOXO transcription factors that regulate responses to oxidative stress and longevity.

In *C. elegans* the TOR pathway also regulates oxidative-stress processes and lifespan. Therefore, we wondered if both cascades are connected. To test this hypothesis we performed epistasis experiments in *C. elegans* analyzing larval arrest and lifespan.

#### 4.4.1 Knockdown of *cst-1* partially suppresses *let-363* L3-arrest phenotype

To investigate a potential connection between *let-363* and *cst-1*, we first assayed if knockdown of *cst-1* can modulate the larval arrest phenotype resulting from loss of *let-363/CeTOR* function. Therefore, *rrf-3(pk1426)* mutants were fed simultaneously with RNAi against *let-363* (pBY1934) and *cst-1* by mixing the dsRNA-expressing *E. coli* cultures.

Reduction of *let-363* function by RNAi resulted in almost complete arrest at the L3 larval stage, while worms fed with *cst-1*RNAi developed normally (Fig. 21 and Tab. 6). Surprisingly, simultaneous feeding of RNAi against *cst-1* and *let-363* partially reversed defective larval development of *let-363*RNAi-treated worms, as 44% of the worms reached adulthood. To exclude the possibility that this could be a concentration-dependent effect caused by dilution of the RNAi-expressing bacteria, both *let-363*RNAi and *cst-1*RNAi cultures were mixed with control bacteria. After mixing, the effect of *let-363*RNAi was only slightly diminished, since only 14% of the worms did not arrest development and reached adulthood. Again, mixing *cst-1*RNAi bacteria with control had no effect on the worms. Together, this indicates a genetic interaction between *let-363* and *cst-1* in the regulation of larval development.

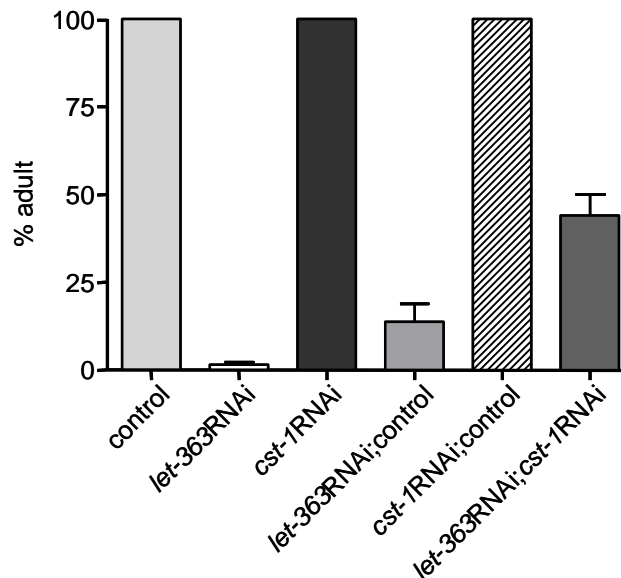


Figure 21. Knockdown of *cst-1* partially suppressed *let-363*RNAi L3-arrest phenotype. Feeding RNAi against *let-363* to *rrf-3(pk1426)* mutants resulted in disruption of larval development and arrest at the L3 stage. This could be partially reversed by RNAi-mediated *cst-1* knockdown. Representation of arrest experiment 1 shown in table 6.

	Experiment 1		Experiment 2		Experiment 3	
	% adults	<i>n</i>	% adults	<i>n</i>	% adults	<i>n</i>
<b>control</b>	100%	167	100%	412	100%	160
<b><i>let-363</i>RNAi</b>	1%	246	17%	405	4%	201
<b><i>cst-1</i>RNAi</b>	100%	256	95%	337	91%	188
<b><i>let-363</i>RNAi;control</b>	14%	182	28%	390	32%	188
<b><i>cst-1</i>RNAi;control</b>	100%	173	92%	391	100%	203
<b><i>let-363</i>RNAi;<i>cst-1</i>RNAi</b>	44%	277	40%	362	60%	181
<i>P</i> -value	0.0006		0.0263		0.1084	

Table 6. *cst-1* modulates the effect of *let-363* on development. The results of three independent larval-arrest tests are presented in this table. Data is listed as: *n* represents number of animals observed; *P*-values refer to *let-363*RNAi;control versus *let-363*RNAi;*cst-1*RNAi animals. Although the difference in experiment number 3 is not significant, the tendency is the same observed in other assays. Worms that crawled off the plates were censored.

#### 4.4.2 Knockout of *cst-1* suppresses *let-363* extended lifespan phenotype

Next we tested whether the long-lived phenotype of *let-363*RNAi-treated worms also depends on *cst-1*. In this lifespan experiment we used a *cst-1(tm1900)* mutant strain (kindly provided by S. Mitani, Japan), which bears a 578 bp deletion and most probably represents a null allele. To rule out the possibility that the *cst-1* mutant phenotype could be produced by undesired mutations in the *C. elegans* genome, the strain was first outcrossed with wild-type (Fig. 8). *cst-1(tm1900)* mutant worms manifested premature signs of aging and 30% reduced lifespan compared with wild-type worms (wild-type mean lifespan =  $16 \pm 0.54$  days; *cst-1(tm1900)* mean lifespan =  $11.2 \pm 0.32$  days) (Fig. 21 and Tab. 7). Similar effects have been observed in previous RNAi experiments, where the lifespan of *cst-1*RNAi-treated worms was reduced by approximately 18% (49).

Reduction of *let-363* function in wild-type worms by RNAi extended mean adult lifespan by 35% (*let-363*RNAi mean lifespan =  $21.6 \pm 0.54$  days). *cst-1(tm1900);let-363*RNAi worms showed a lifespan elongation of 24% compared to *cst-1(tm1900)* (*cst-1(tm1900);let-363*RNAi mean lifespan =  $13.9 \pm 0.43$  days). This indicates that knockout of *cst-1* can partially suppress the extended lifespan of *let-363*RNAi. From these observations we conclude that *cst-1* is epistatic to *let-363*, and might modulate, at least in part, *let-363* function.

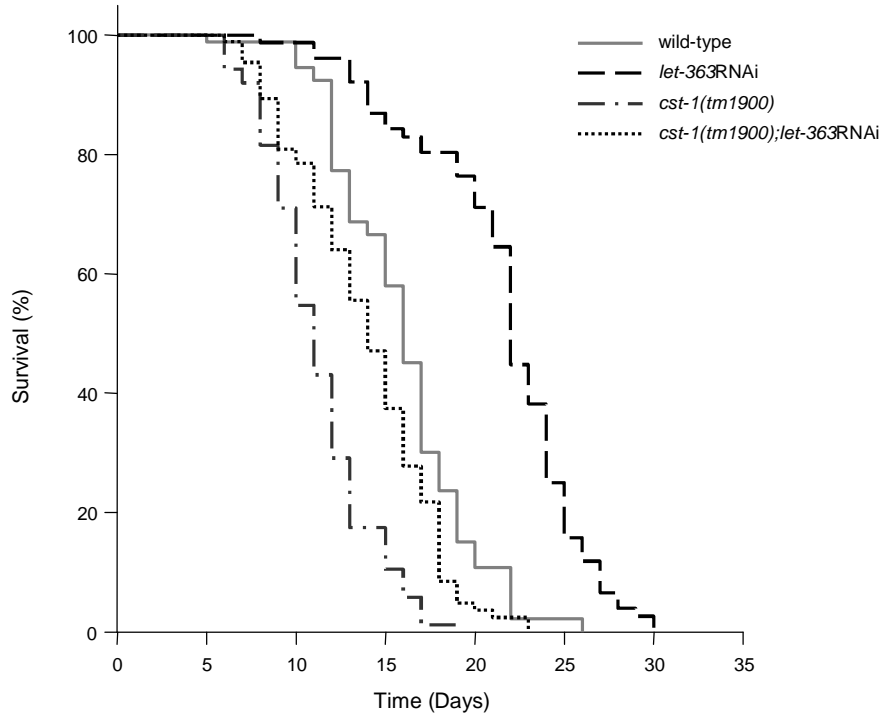


Figure 22. *cst-1* is required for the lifespan extension of *let-363RNAi* treated worms. Lifespan analysis of *let-363RNAi*, *cst-1(tm1900)* and *cst-1(tm1900);let-363RNAi* at 20°C. Feeding RNAi against *let-363* to wild-type worms results in extended lifespan. *cst-1* knockout caused by the mutation *cst-1(tm1900)* partially suppresses this phenotype. Representation of lifespan experiment 1 shown in table 7.

		wild-type	<i>let-363RNAi</i>	<i>cst-1(tm1900)</i>	<i>cst-1(tm1900);let-363RNAi</i>
1	mean lifespan	16 ± 0.54	21.6 ± 0.54	11.2 ± 0.32	13.9 ± 0.43
	<i>n</i>	100	100	100	100
	<i>P</i> -value		<0.001	<0.001	0.014
2	mean lifespan	14.6 ± 0.31	19.6 ± 0.43	7.8 ± 0.27	10.8 ± 0.41
	<i>n</i>	125	126	122	127
	<i>P</i> -value		<0.001	<0.001	<0.001
3	mean lifespan	15.9 ± 0.33	19.7 ± 0.36	10.6 ± 0.26	11.6 ± 0.33
	<i>n</i>	100	100	101	100
	<i>P</i> -value		<0.001	<0.001	<0.001

Table 7. *cst-1* modulates the effect of *let-363* on lifespan. The results of three independent lifespan assays are presented in this table. Data is listed as: mean lifespan (days) ± standard error of the mean; *n* represents number of animals observed; *P*-values refer to experimental strain and wild-type control animals. Worms that displayed Egl-phenotype, extruded organs and crawled off the plate were censored.

## 5. Discussion

### 5.1 Expression analysis of *let-363/CeTOR*

#### 5.1.1 *let-363/CeTOR* locates in an operon and is expressed together with and downstream of the mitochondrial ribosomal protein B0261.4

In the first part of this study we analyzed the transcriptional regulation of *let-363* and its site of gene function. Our RT-PCR study revealed that the *let-363* mRNA bears predominantly the SL2 sequence at its 5' end, indicating that *let-363* is *trans*-spliced in an SL2 manner and resides in a cluster of genes. Clustering of genes in operons and *trans*-splicing is a characteristic feature of nematodes. The gene cluster is transcribed from a promoter and regulatory sequence at the 5' end of the cluster. The polycistronic pre-mRNA is then converted into monocistronic mRNAs by cleavage and polyadenylation at the 3' ends of the upstream genes accompanied by SL2-specific *trans*-splicing of the downstream genes (7, 9). Furthermore, genes in an operon are quite close together, in most cases the 3' end of the upstream gene and the 5' end of the downstream gene are about 100 to 1,000 bp apart. Here, the distance between *let-363* and the upstream gene B0261.4 is 488 bp, supporting our hypothesis that *let-363* resides in an operon. For the same reason, the gene B0261.1, which lays 703 bp downstream of *let-363*, is predicted to be part of the same operon.

Interestingly, *let-363* mRNA not only received the SL2, but also the SL1. This has been described before for other genes in downstream positions (82, 103). However, *trans*-splice sites near promoters accept only SL1 (13, 103). Why some downstream genes receive a mixture of SL1 and SL2 is not clear yet. One possibility is that these operons have internal promoters, so the SL1 containing *let-363* message might arise from pre-mRNA started at an internal promoter.

It is generally accepted that in *C. elegans* operons serve an important regulatory purpose: they allow co-expression from a single promoter of genes whose products function together (7, 8). Thus, the arrangement of *let-363* and B0261.4 in an operon could be the first link for a co-regulation of both genes. By protein sequence alignments we identified B0261.4 as the *C. elegans* orthologue of the human mitochondrial ribosomal protein L47 (MRP-L47). Indeed, the mTOR pathway

regulates translational processes and ribosome biogenesis (26, 98). Therefore, their presence together in the operon might serve the purpose of co-expression in the cell and coordinate their functions. In addition, B0261.1 encodes a subunit of the transcription initiation factor TFIIIB (97), supporting the idea of a possible functional connection of the co-expressed genes residing in the operon. However, future genetic and biochemical studies have to be undertaken to clarify this connection in more detail.

### **5.1.2 *let-363/CeTOR* is strongly expressed in tissues that regulate development through sensing the nutritional status**

The findings that the *let-363* locates in an operon and its pre-mRNA is SL2 spliced suggest that the entire gene cluster is transcribed from a single promoter upstream of the first gene B0261.4. Therefore, we assessed the promoter and regulatory regions for *let-363* expression by translational fusion of gene sequences to GFP and transformation in *C. elegans*.

The full expression pattern of *let-363* was observed with the construct P3, containing 3.9 Kbp upstream regulatory sequence. *let-363* was expressed ubiquitously throughout all developmental stages, including embryonic development. GFP staining was strongly observed in head and tail neurons, all segments of the pharynx, intestine, vulva, spermatheca, distal tip cells, somatic muscle and hypodermis.

Different segments in this 3.9 Kbp region seemed to be responsible for its expression in different tissues. The 2.5 Kbp region 5' of B0261.4 (construct P2) drove expression in all developmental stages. Assuming that this region includes the promoter of the operon, this sequence might be sufficient for timing the expression of *let-363*.

Interestingly, the 500 bp region directly upstream of *let-363* (construct P1) drove strong expression in head and tail neurons, all segments of the pharynx and intestinal cells, tissues which are important for amino acid and energy homeostasis, two of the main inputs that regulate CeTOR activity.

CeTOR signaling is necessary for proper intestinal function, since null mutations in CeTOR lead to remarkable intestine atrophy (54). Sensing of nutrient availability in the intestine e.g. through the intestinal oligopeptide transporter PEP-2 might be an important regulatory input on CeTOR activity (57). A role for CeTOR in regulation of nutrient and energy homeostasis is further supported by its expression in the ASI

neurons, two neuronal cells situated in the head. Their single ciliated dendrites extend into and are part of the amphids, the principal chemosensory organs in nematodes (96). Furthermore, they render critical information about food availability to diverse endocrine signals responsible for the regulation of development, metabolism, and aging (4). Here insulin/IGF and TGF $\beta$  signaling might cross-talk with the TOR pathway to adapt development and metabolism to environmental conditions (102).

Together, the short regulatory sequence directly upstream of *let-363* might function as an internal promoter and ensure proper spatial expression in critical tissues, while the regulatory sequence of the operon regulates temporal expression. This would also explain why *let-363* mRNA is sliced to a mixture of SL2 and SL1: the SL2-containing *let-363* message arises from the general operon promoter while the SL1 pre-mRNA is started at an internal promoter.

It is important to remark that the result obtained with transcriptional reporters bears limitations and might not represent the real expression pattern. By introducing reporter sequences into *C. elegans* genes, control signals could be disrupted. The generation of multi-copy arrays leads to overexpression which can result in ectopic expression in particular cells and the possibility of mosaic loss of the transforming array is a source of uncertainty (59). Furthermore, GFP can circulate through cellular compartments, meaning stronger fluorescence in certain parts of the cells does not necessarily mean stronger expression or specific localization. Therefore, to verify the *let-363* expression pattern obtained in this study by transcriptional reporter analysis independent means should be used next. Comparison with *in situ* hybridization and antibody staining can give additional information about the expression and localization of the endogenous protein in the organism.

These data can be used for further analysis of the *let-363/CeTOR* regulatory network. With the identification of regulatory elements in *let-363* promoter the question arises which transcription factors do operate in this network. Can changes in the local environment influence the cellular expression pattern? Furthermore, the specification of the *let-363* promoter can provide important cues for the generation of a translational reporter to analyze the site of CeTOR function in more detail and to perform cell-type specific rescue experiments.

## 5.2 Search for CeTOR genetic interactors by genome-wide RNAi screening

One of the most ambitious approaches for genetic analysis in *C. elegans* has been the discovery of RNA-mediated interference (RNAi), a technique that allows efficient inactivation of specific targeted genes (20). In the last years, RNAi screening methods have emerged that allow fast and efficient genome wide screening of *C. elegans* (40). Using an RNAi feeding library composed of more than 16,700 single *E. coli* clones expressing dsRNA we can screen most of the predicted *C. elegans* genes. In this study we developed a strategy for a genome-wide RNAi screen to search systematically for genes affecting TOR developmental functions.

For RNAi screening purposes, we first generated a stable *let-363* mutant strain. By microinjection and transformation we introduced the entire *let-363/CeTOR* wild-type coding sequence together with the fluorescent marker *myo-2P::gfp* as extrachromosomal array in *let-363* mutants. This strain segregated in transgenic worms bearing the extrachromosomal array and non-transgenic animals. The wild-type *let-363* array, easily recognizable by the fluorescent marker, complemented the mutant phenotype and allowed normal development to reproductive adults, while non-transgenic worms displayed the full mutant phenotype and arrested larval development at the L3 stage. With this strain it was possible to keep the otherwise lethal *let-363* mutants alive. Furthermore, to increase the sensitivity of *let-363* mutants to RNAi and thus induce stronger RNAi phenotypes we introduced a mutation in *rrf-3* in our mutant strain (80).

The larval arrest provided a simple and convenient assay with which to identify genes that regulate *let-363* function. We expected that knockdown of target genes by RNAi could have an effect on the developmental block in *let-363* mutants and induce progression to adulthood. In this context, a complete or partial rescue of the L3-arrest phenotype of *let-363* mutants would denote a genetic interaction between *let-363* and the RNAi-targeted gene.

Next, the screening protocol was optimized to ensure the best conditions before embarking on large-scale screens. In a pilot screen we tested 48 clones from the *C. elegans* RNAi feeding library. However, inhibition of these genes by RNAi did not result in suppression of the TOR mutant phenotype. Using the protocol established in this study we can now assay the whole library of approximately 16,700 RNAi-feeding



clones screening 86% of the *C. elegans* genome. Given the importance of CeTOR for normal development and the complexity of the processes influenced by this pathway, it seems reasonable to expect that RNAi-induced withdrawal of one gene may compensate the lack of CeTOR signaling only partially. Keeping this in mind, worms in the screening need to be carefully examined for incomplete rescue of the developmental arrest phenotype. Bacterial clones that produce “hits” in the primary screen should be re-screened an additional time to confirm the result. With this approach we expect to uncover novel upstream and downstream genes involved in TOR signaling. The screen should also identify known genes in the TOR pathway (positive control). The function of candidate genes in the TOR pathway can be tested next using the *C. elegans* genetics and biochemical methods.

### **5.3 *let-363/CeTOR* interacts with *cst-1*, the *C. elegans* orthologue of *MST1* in the mammalian Hippo pathway**

A substantial body of evidence has demonstrated the importance of TOR signaling for the regulation of metabolism and cell growth in response to nutrients and hormone-dependent signals (98). In *C. elegans*, TOR is a major regulator of reproductive growth, stress response and aging (54). There is evidence of a cross-talk between insulin/IGF signaling and CeTOR at several levels. Remarkably, loss of CeTOR function extends lifespan and this effect was not enhanced by insulin receptor mutants (37, 93). However, little is known about the role of other genetic pathways in the regulation of CeTOR.

Additional input to the regulation of oxidative stress response and lifespan is conferred by the evolutionary conserved MST/Hippo pathway (49). We demonstrate here that *cst-1*, the *C. elegans* orthologue of MST1, acts as modulator of CeTOR-mediated developmental processes and longevity. Mutation of *cst-1* suppressed the extended lifespan of *let-363* deprived worms. Moreover, loss of *cst-1* partially suppressed the developmental defect of *let-363*RNAi mediated knockdown.

Together, these data suggest that the CST pathway genetically interacts with the CeTOR pathway in the control of longevity and development. However, CeTOR and *cst-1* have opposing effects in *C. elegans*: loss of *let-363/CeTOR* delayed aging while knockout of the *cst-1* accelerated aging and promoted enhanced stress sensitivity

(49). Similarly, in mammals and *Drosophila*, evidence suggests that both pathways antagonize in the control of cell growth (19).

Our preliminary data suggest that active *cst-1* is required for lifespan extension of *let-363* knockdown. Since *cst-1* mutation efficiently suppressed *let-363* longevity and developmental arrest, we propose a model in which *cst-1* is genetically positioned downstream of CeTOR. Interestingly, our *cst-1* deletion mutant did not completely abolish *let-363* extended longevity. In mammals MST1 acts in a complex with MST2. Since MST/hippo signaling is evolutionary conserved we assume that *cst-2*, the *C. elegans* orthologue of MST2 still retains some degree of activity. In this context, it would be interesting to test if *cst-2* can phenocopy *cst-1* and if knockout of both *cst* genes can completely suppress *let-363*RNAi-mediated lifespan extension.

Another explanation might be that *cst-1* functions upstream of CeTOR. Together with the opposing phenotypes of *cst-1* and *let-363* mutants, our results might suggest that *cst-1* negatively affects *let-363*/CeTOR functions. In this model, absence of *cst-1* results in the upregulation of CeTOR function. This could explain the partial compensation of *let-363*RNAi-mediated larval arrest by knockdown of *cst-1*. It is important to note that feeding RNAi does not produce a complete knockout of the targeted gene. Therefore, remaining levels of CeTOR can still be activated in the background of reduced *cst-1* function.

This study reveals a novel genetic link between Hippo/CST and CeTOR signaling in *C. elegans*. However, the exact genetic order still remains elusive. How *cst-1* interacts with *let-363*/CeTOR needs to be determined in future studies. Epistasis experiments with single and double mutants as well as overexpression experiments will help to define the genetic interaction. Of special interest is the question which TOR complex, TORC1 or TORC2, contributes to this signal transduction. TORC1 is composed of DAF-15/CeRaptor and L-ST8, while RICT-1/CeRictor has been recently described as component of TORC2 in *C. elegans* (37, 39, 81). Genetic experiments with *cst-1* and the main components of both TOR complexes, *daf-15*/CeRaptor and *rict-1*/CeRictor, will help to distinguish which complex is involved.

## 5.4 Conclusions

The aim of this study was to present the model organism *C. elegans* as a powerful laboratory instrument for the investigation of the TOR signaling pathway. Unraveling new mechanisms involved in its regulation and effects, we are trying to better understand the events underlying cyst formation and disease progression in ADPKD, with the hope of helping in the development of new therapies for this until now intractable syndrome. With three different approaches (expression analysis, genome-wide search of interactors, and finding a novel genetic interaction between the TOR and the Hippo pathway) we have shown that the worm is a very versatile tool suitable for further investigation of the TOR signaling pathway and of ADPKD pathogenesis.

## 6. Appendix

### Enzymes and kits

Gene Ruler™ 100+500bp DNA Ladder	Fermentas GmbH
Gene Ruler™ 1 kb DNA Ladder	Fermentas GmbH
6x DNA Loading Dye	Fermentas GmbH
KOD Hot Start DNA Polymerase	Merck KGaA
Taq DNA Polymerase	Genaxxon BioScience GmbH
OptiTaq DNA Polymerase	Genaxxon BioScience GmbH
Superscript III Reverse Transcriptase	Invitrogen GmbH
Proteinase K	Sigma-Aldrich Chemie GmbH
Restriction enzymes	New England Biolabs GmbH
Alkaline Phosphatase CIAP	USB Europe GmbH
T4 DNA Ligase	Fermentas GmbH
NucleoBond® Xtra Maxi Kit	Macherey-Nagel GmbH
QIAprep® Spin Miniprep Kit	Qiagen
QIAquick® PCR Purification Kit	Qiagen
QIAquick® Gel Extraction Kit	Qiagen
RNeasy® Mini Kit	Qiagen

### Devices and equipment

#### Microscopes:

AxioCam MRm digital camera	Carl Zeiss AG
Axioplan2 fluorescence microscope	Carl Zeiss AG
Fluorescence microscope Imager Z1	Carl Zeiss AG
MZ 16 F microscope	Leica Microsystems GmbH
MZ 9.5 microscope	Leica Microsystems GmbH
SZX7 microscope	Olympus

#### Centrifuges:

Biofuge fresco centrifuge	Heraeus Holding GmbH
Megafuge 3.0 R centrifuge	Heraeus Holding GmbH
5417 R centrifuge	Eppendorf
J6-MI centrifuge	Beckman Coulter
Perfect Spin24 centrifuge	Peqlab Biotechnologie GmbH
RC6Plus centrifuge	Sorvall-Thermo Fisher Scientific
SLA-1500 rotor	Thermo Fisher Scientific

#### Electrophoresis:

E835 power supply	Consort
EPS 3500 XL power supply	Amersham Pharmacia Biotech
PowerPac basic/universal power supply	BioRad Laboratories

#### Thermal cyclers:

PTC-200 thermal gradient cycler	MJ Research
---------------------------------	-------------

#### Incubators:

BD115 incubator	Binder GmbH
Heraeus function line B6 and B20 incubators	Heraeus Holding GmbH
Innova 4430 and 4300 incubator shakers	New Brunswick Scientific

#### Miscellaneous:

DMZ-universal needle puller	Zeitz Instrumente GmbH
FemtoJet express microinjector	Eppendorf
Spectramax plus 384 spectrophotometer	MDS Analytical Devices
Dri-Block heater DB-2A	Techne AG
Thermomixer comfort	Eppendorf
Intellimixer overhead shaker	Fröbel Labortechnik
LP62005 and BP121S balances	Satorius AG
Coolpix 990 camera	Nikon

## 7. Abbreviations

°C	Degrees Celsius
%	Percent
∅	Diameter
µg	Microgram
µl	Microliter
µm	Micrometer
4E-BP1	Eukaryotic translation initiation factor 4E binding protein 1
ADPKD	Autosomal dominant polycystic kidney disease
Amp	Ampicillin
AMP	Adenosine monophosphate
AMPK	AMP-activated kinase
ATP	Adenosine triphosphate
bp	Base-pairs
C-	Carboxyl
<i>C. elegans</i>	<i>Caenorhabditis elegans</i>
cDNA	Coding DNA
CeTOR	<i>C. elegans</i> target of rapamycin
CeTORC	CeTOR complex
COPAS	Complex Object Parametric Analyzer and Sorter
CSC	The <i>C. elegans</i> Sequencing Consortium
CST	<i>Caenorhabditis</i> STE20-like kinase
CT	Computed tomography
DAF	Abnormal dauer formation
ddH <sub>2</sub> O	double distilled H <sub>2</sub> O
DIC	Differential interference contrast
DMSO	Dimethyl sulfoxide
DNA	Deoxyribonucleic acid
DPY	Dumpy
dsRNA	Double-stranded RNA
<i>E. coli</i>	<i>Escherichia coli</i>
e.g.	<i>exempli gratia</i> (eng.: for example)
EDTA	Ethylenediaminetetraacetic acid
EGFP	Endow GFP
egl	Egg-laying defective
<i>et al.</i>	<i>et alii</i> (eng.: and others)
EtOH	Ethanol
Ex	Extrachromosomal
F1-F4	<i>C. elegans</i> generation 1-4
FKBP12	12-kDa FK506-binding protein
Fig.	Figure
g	Gram
GAP	GTPase activating protein
GDP	Guanosine diphosphate
GTP	Guanosine triphosphate
IGF	Insulin-like growth factor
IPTG	Isopropyl-β-D-thiogalactopyranoside
IRS	Insulin receptor substrate
Kan	Kanamycin
Kbp	Kilo base-pairs
l	Liter
L1-L4	<i>C. elegans</i> larval stages 1-4
LB	Luria-Bertani
LET	Lethal
M	Molar
mg	Milligram
min	Minute
ml	Milliliter

mM	Millimolar
mm	Millimeter
mRNA	Messenger RNA
mTOR	Mammalian target of Rapamycin
mTORC	mTOR complex
MR	Magnetic resonance
MST	Mammalian sterile twenty
MYO	Myosin heavy chain structural genes
N-	Amino
ng	Nanogram
NGM	Nematode growth medium
nM	Nanomolar
P1	<i>let-363</i> promoter construct 1
P2	<i>let-363</i> promoter construct 2
P3	<i>let-363</i> promoter construct 3
PC	Polycystin
PCP	Planar cell polarity
PCR	Polymerase chain reaction
PEP-2	<i>C. elegans</i> peptide transporter 2
PIKK	Phosphatidylinositol kinase-related kinase
PI3K	Phosphoinositide-3-kinase
PKD	Polycystic kidney disease
Raptor	Regulatory-associated protein of TOR
Rheb	Ras homolog enriched in brain
Rictor	Rapamycin-insensitive companion of mTOR
RNA	Ribonucleic acid
RNAi	RNA interference
ROL	Roller
RRF	RNA-dependent RNA polymerase family
rRNA	Ribosomal RNA
RT-PCR	Reverse transcriptase PCR
S6K1	Ribosomal S6 kinase 1
SL	Spliced leader
Tab.	Table
Tet	Tetracycline
TOP	Terminal oligopyrimidine
TOR	Target of Rapamycin
TRP	Transient receptor potential
TSC	Tuberous sclerosis
UNC	Uncoordinated
UV	Ultraviolet
Wnt	Wingless-type
WT	Wild-type

## 8. References

1. **Aguiari, G., V. Trimi, M. Bogo, A. Mangolini, G. Szabadkai, P. Pinton, R. Witzgall, P. C. Harris, P. A. Borea, R. Rizzuto, and L. del Senno.** (2008). Novel role for polycystin-1 in modulating cell proliferation through calcium oscillations in kidney cells. *Cell Prolif* 41:554-73.
2. **Ahringer, J., ed.** . (2006). Reverse genetics. *WormBook*, ed. The *C. elegans* Research Community, WormBook, doi/10.1895/wormbook.1.47.1, <http://www.wormbook.org>.
3. **Bai, X., and Y. Jiang.** (2010). Key factors in mTOR regulation. *Cell Mol Life Sci* 67:239-53.
4. **Bargmann, C. I., and H. R. Horvitz.** (1991). Control of larval development by chemosensory neurons in *Caenorhabditis elegans*. *Science* 251:1243-6.
5. **Baumeister, R., E. Schaffitzel, and M. Hertweck.** (2006). Endocrine signaling in *Caenorhabditis elegans* controls stress response and longevity. *J Endocrinol* 190:191-202.
6. **Bennett, W. M.** (2009). Autosomal dominant polycystic kidney disease: 2009 update for internists. *Korean J Intern Med* 24:165-8.
7. **Blumenthal, T.** (2005). Trans-splicing and operons. *WormBook*:1-9.
8. **Blumenthal, T., and K. S. Gleason.** (2003). *Caenorhabditis elegans* operons: form and function. *Nat Rev Genet* 4:112-20.
9. **Blumenthal, T., and K. Steward.** (1997). *C. elegans* II, chapter 6: RNA Processing and Gene Structure., Donald L. Riddle, Thomas Blumenthal, Barbara J. Meyer and James R. Priess ed. Cold Spring Harbor Laboratory Press, New York.
10. **Brenner, S.** (1974). The genetics of *Caenorhabditis elegans*. *Genetics* 77:71-94.
11. **Brook-Carter, P. T., B. Peral, C. J. Ward, P. Thompson, J. Hughes, M. M. Maheshwar, M. Nellist, V. Gamble, P. C. Harris, and J. R. Sampson.** (1994). Deletion of the TSC2 and PKD1 genes associated with severe infantile polycystic kidney disease--a contiguous gene syndrome. *Nat Genet* 8:328-32.
12. **Chan, E. Y.** (2009). mTORC1 phosphorylates the ULK1-mAtg13-FIP200 autophagy regulatory complex. *Sci Signal* 2:pe51.
13. **Conrad, R., K. Lea, and T. Blumenthal.** (1995). SL1 trans-splicing specified by AU-rich synthetic RNA inserted at the 5' end of *Caenorhabditis elegans* pre-mRNA. *Rna* 1:164-70.
14. **Corsi, A. K.** (2006). A biochemist's guide to *Caenorhabditis elegans*. *Anal Biochem* 359:1-17.
15. **CSC.** (1998). Genome sequence of the nematode *C. elegans*: a platform for investigating biology. *Science* 282:2012-8.
16. **Deane, J. A., and S. D. Ricardo.** (2007). Polycystic kidney disease and the renal cilium. *Nephrology (Carlton)* 12:559-64.
17. **Dere, R., P. D. Wilson, R. N. Sandford, and C. L. Walker.** (2010). Carboxy terminal tail of polycystin-1 regulates localization of TSC2 to repress mTOR. *PLoS One* 5:e9239.

18. **Dibble, C. C., J. M. Asara, and B. D. Manning.** (2009). Characterization of Rictor phosphorylation sites reveals direct regulation of mTOR complex 2 by S6K1. *Mol Cell Biol* 29:5657-70.
19. **Dong, J., G. Feldmann, J. Huang, S. Wu, N. Zhang, S. A. Comerford, M. F. Gayyed, R. A. Anders, A. Maitra, and D. Pan.** (2007). Elucidation of a universal size-control mechanism in *Drosophila* and mammals. *Cell* 130:1120-33.
20. **Fire, A., S. Xu, M. K. Montgomery, S. A. Kostas, S. E. Driver, and C. C. Mello.** (1998). Potent and specific genetic interference by double-stranded RNA in *Caenorhabditis elegans*. *Nature* 391:806-11.
21. **Fraser, A. G., R. S. Kamath, P. Zipperlen, M. Martinez-Campos, M. Sohrmann, and J. Ahringer.** (2000). Functional genomic analysis of *C. elegans* chromosome I by systematic RNA interference. *Nature* 408:325-30.
22. **Gonzalez-Perrett, S., K. Kim, C. Ibarra, A. E. Damiano, E. Zotta, M. Batelli, P. C. Harris, I. L. Reisin, M. A. Arnaout, and H. F. Cantiello.** (2001). Polycystin-2, the protein mutated in autosomal dominant polycystic kidney disease (ADPKD), is a Ca<sup>2+</sup>-permeable nonselective cation channel. *Proc Natl Acad Sci U S A* 98:1182-7.
23. **Guertin, D. A., D. M. Stevens, C. C. Thoreen, A. A. Burds, N. Y. Kalaany, J. Moffat, M. Brown, K. J. Fitzgerald, and D. M. Sabatini.** (2006). Ablation in mice of the mTORC components raptor, rictor, or mLST8 reveals that mTORC2 is required for signaling to Akt-FOXO and PKCalpha, but not S6K1. *Dev Cell* 11:859-71.
24. **Gwinn, D. M., D. B. Shackelford, D. F. Egan, M. M. Mihaylova, A. Mery, D. S. Vasquez, B. E. Turk, and R. J. Shaw.** (2008). AMPK phosphorylation of raptor mediates a metabolic checkpoint. *Mol Cell* 30:214-26.
25. **Hansen, M., A. Chandra, L. L. Mitic, B. Onken, M. Driscoll, and C. Kenyon.** (2008). A role for autophagy in the extension of lifespan by dietary restriction in *C. elegans*. *PLoS Genet* 4:e24.
26. **Hansen, M., S. Taubert, D. Crawford, N. Libina, S. J. Lee, and C. Kenyon.** (2007). Lifespan extension by conditions that inhibit translation in *Caenorhabditis elegans*. *Aging Cell* 6:95-110.
27. **Hara, K., Y. Maruki, X. Long, K. Yoshino, N. Oshiro, S. Hidayat, C. Tokunaga, J. Avruch, and K. Yonezawa.** (2002). Raptor, a binding partner of target of rapamycin (TOR), mediates TOR action. *Cell* 110:177-89.
28. **Harris, P. C., and V. E. Torres.** (2009). Polycystic kidney disease. *Annu Rev Med* 60:321-37.
29. **Henderson, S. T., M. Bonafe, and T. E. Johnson.** (2006). *daf-16* protects the nematode *Caenorhabditis elegans* during food deprivation. *J Gerontol A Biol Sci Med Sci* 61:444-60.
30. **Hertweck, M., C. Gobel, and R. Baumeister.** (2004). *C. elegans* SGK-1 is the critical component in the Akt/PKB kinase complex to control stress response and life span. *Dev Cell* 6:577-88.
31. **Honjoh, S., T. Yamamoto, M. Uno, and E. Nishida.** (2009). Signalling through RHEB-1 mediates intermittent fasting-induced longevity in *C. elegans*. *Nature* 457:726-30.
32. **Hughes, J., C. J. Ward, B. Peral, R. Aspinwall, K. Clark, J. L. San Millan, V. Gamble, and P. C. Harris.** (1995). The polycystic kidney disease 1 (PKD1) gene encodes a novel protein with multiple cell recognition domains. *Nat Genet* 10:151-60.
33. **Inoki, K., T. Zhu, and K. L. Guan.** (2003). TSC2 mediates cellular energy response to control cell growth and survival. *Cell* 115:577-90.



34. **Jacinto, E., R. Loewith, A. Schmidt, S. Lin, M. A. Ruegg, A. Hall, and M. N. Hall.** (2004). Mammalian TOR complex 2 controls the actin cytoskeleton and is rapamycin insensitive. *Nat Cell Biol* 6:1122-8.
35. **Jacinto, E., and A. Lorberg.** (2008). TOR regulation of AGC kinases in yeast and mammals. *Biochem J* 410:19-37.
36. **Jastrzebski, K., K. M. Hannan, E. B. Tchoubrieva, R. D. Hannan, and R. B. Pearson.** (2007). Coordinate regulation of ribosome biogenesis and function by the ribosomal protein S6 kinase, a key mediator of mTOR function. *Growth Factors* 25:209-26.
37. **Jia, K., D. Chen, and D. L. Riddle.** (2004). The TOR pathway interacts with the insulin signaling pathway to regulate *C. elegans* larval development, metabolism and life span. *Development* 131:3897-906.
38. **Jiang, S. T., Y. Y. Chiou, E. Wang, H. K. Lin, Y. T. Lin, Y. C. Chi, C. K. Wang, M. J. Tang, and H. Li.** (2006). Defining a link with autosomal-dominant polycystic kidney disease in mice with congenitally low expression of Pkd1. *Am J Pathol* 168:205-20.
39. **Jones, K. T., E. R. Greer, D. Pearce, and K. Ashrafi.** (2009). Rictor/TORC2 regulates *Caenorhabditis elegans* fat storage, body size, and development through sgk-1. *PLoS Biol* 7:e60.
40. **Kamath, R. S., and J. Ahringer.** (2003). Genome-wide RNAi screening in *Caenorhabditis elegans*. *Methods* 30:313-21.
41. **Kamath, R. S., A. G. Fraser, Y. Dong, G. Poulin, R. Durbin, M. Gotta, A. Kanapin, N. Le Bot, S. Moreno, M. Sohrmann, D. P. Welchman, P. Zipperlen, and J. Ahringer.** (2003). Systematic functional analysis of the *Caenorhabditis elegans* genome using RNAi. *Nature* 421:231-7.
42. **Kenyon, C., J. Chang, E. Gensch, A. Rudner, and R. Tabtiang.** (1993). A *C. elegans* mutant that lives twice as long as wild type. *Nature* 366:461-4.
43. **Kim, D. H., D. D. Sarbassov, S. M. Ali, J. E. King, R. R. Latek, H. Erdjument-Bromage, P. Tempst, and D. M. Sabatini.** (2002). mTOR interacts with raptor to form a nutrient-sensitive complex that signals to the cell growth machinery. *Cell* 110:163-75.
44. **Kim, D. H., D. D. Sarbassov, S. M. Ali, R. R. Latek, K. V. Guntur, H. Erdjument-Bromage, P. Tempst, and D. M. Sabatini.** (2003). GbetaL, a positive regulator of the rapamycin-sensitive pathway required for the nutrient-sensitive interaction between raptor and mTOR. *Mol Cell* 11:895-904.
45. **Kim, E., and K. L. Guan.** (2009). RAG GTPases in nutrient-mediated TOR signaling pathway. *Cell Cycle* 8:1014-8.
46. **Kimura, K. D., H. A. Tissenbaum, Y. Liu, and G. Ruvkun.** (1997). *daf-2*, an insulin receptor-like gene that regulates longevity and diapause in *Caenorhabditis elegans*. *Science* 277:942-6.
47. **Lee, R. Y., J. Hench, and G. Ruvkun.** (2001). Regulation of *C. elegans* DAF-16 and its human ortholog FKHL1 by the *daf-2* insulin-like signaling pathway. *Curr Biol* 11:1950-7.
48. **Lehner, B., J. Tischler, and A. G. Fraser.** (2006). RNAi screens in *Caenorhabditis elegans* in a 96-well liquid format and their application to the systematic identification of genetic interactions. *Nat Protoc* 1:1617-20.
49. **Lehtinen, M. K., Z. Yuan, P. R. Boag, Y. Yang, J. Villen, E. B. Becker, S. DiBacco, N. de la Iglesia, S. Gygi, T. K. Blackwell, and A. Bonni.** (2006). A conserved MST-FOXO signaling pathway mediates oxidative-stress responses and extends life span. *Cell* 125:987-1001.

50. **Leung, A. K., and W. L. Robson.** (2007). Tuberous sclerosis complex: a review. *J Pediatr Health Care* 21:108-14.
51. **Lewis, J. A., and J. T. Fleming.** (1995). Basic culture methods. *Methods Cell Biol* 48:3-29.
52. **Lin, K., J. B. Dorman, A. Rodan, and C. Kenyon.** (1997). daf-16: An HNF-3/forkhead family member that can function to double the life-span of *Caenorhabditis elegans*. *Science* 278:1319-22.
53. **Loewith, R., E. Jacinto, S. Wullschleger, A. Lorberg, J. L. Crespo, D. Bonenfant, W. Oppliger, P. Jenoe, and M. N. Hall.** (2002). Two TOR complexes, only one of which is rapamycin sensitive, have distinct roles in cell growth control. *Mol Cell* 10:457-68.
54. **Long, X., C. Spycher, Z. S. Han, A. M. Rose, F. Muller, and J. Avruch.** (2002). TOR deficiency in *C. elegans* causes developmental arrest and intestinal atrophy by inhibition of mRNA translation. *Curr Biol* 12:1448-61.
55. **Ma, X. M., and J. Blenis.** (2009). Molecular mechanisms of mTOR-mediated translational control. *Nat Rev Mol Cell Biol* 10:307-18.
56. **Masoumi, A., B. Reed-Gitomer, C. Kelleher, M. R. Bekheirnia, and R. W. Schrier.** (2008). Developments in the management of autosomal dominant polycystic kidney disease. *Ther Clin Risk Manag* 4:393-407.
57. **Meissner, B., M. Boll, H. Daniel, and R. Baumeister.** (2004). Deletion of the intestinal peptide transporter affects insulin and TOR signaling in *Caenorhabditis elegans*. *J Biol Chem* 279:36739-45.
58. **Melendez, A., Z. Talloczy, M. Seaman, E. L. Eskelinen, D. H. Hall, and B. Levine.** (2003). Autophagy genes are essential for dauer development and life-span extension in *C. elegans*. *Science* 301:1387-91.
59. **Mello, C., and A. Fire.** (1995). DNA transformation. *Methods Cell Biol* 48:451-82.
60. **Mochizuki, T., G. Wu, T. Hayashi, S. L. Xenophontos, B. Veldhuisen, J. J. Saris, D. M. Reynolds, Y. Cai, P. A. Gabow, A. Pierides, W. J. Kimberling, M. H. Breuning, C. C. Deltas, D. J. Peters, and S. Somlo.** (1996). PKD2, a gene for polycystic kidney disease that encodes an integral membrane protein. *Science* 272:1339-42.
61. **Nauli, S. M., F. J. Alenghat, Y. Luo, E. Williams, P. Vassilev, X. Li, A. E. Elia, W. Lu, E. M. Brown, S. J. Quinn, D. E. Ingber, and J. Zhou.** (2003). Polycystins 1 and 2 mediate mechanosensation in the primary cilium of kidney cells. *Nat Genet* 33:129-37.
62. **Nauli, S. M., Y. Kawanabe, J. J. Kaminski, W. J. Pearce, D. E. Ingber, and J. Zhou.** (2008). Endothelial cilia are fluid shear sensors that regulate calcium signaling and nitric oxide production through polycystin-1. *Circulation* 117:1161-71.
63. **Nojima, H., C. Tokunaga, S. Eguchi, N. Oshiro, S. Hidayat, K. Yoshino, K. Hara, N. Tanaka, J. Avruch, and K. Yonezawa.** (2003). The mammalian target of rapamycin (mTOR) partner, raptor, binds the mTOR substrates p70 S6 kinase and 4E-BP1 through their TOR signaling (TOS) motif. *J Biol Chem* 278:15461-4.
64. **Paradis, S., and G. Ruvkun.** (1998). *Caenorhabditis elegans* Akt/PKB transduces insulin receptor-like signals from AGE-1 PI3 kinase to the DAF-16 transcription factor. *Genes Dev* 12:2488-98.
65. **Peterson, T. R., M. Laplante, C. C. Thoreen, Y. Sancak, S. A. Kang, W. M. Kuehl, N. S. Gray, and D. M. Sabatini.** (2009). DEPTOR is an mTOR inhibitor frequently overexpressed in multiple myeloma cells and required for their survival. *Cell* 137:873-86.

66. **Piano, F., A. J. Schetter, M. Mangone, L. Stein, and K. J. Kemphues.** (2000). RNAi analysis of genes expressed in the ovary of *Caenorhabditis elegans*. *Curr Biol* 10:1619-22.
67. **Praitis, V., E. Casey, D. Collar, and J. Austin.** (2001). Creation of low-copy integrated transgenic lines in *Caenorhabditis elegans*. *Genetics* 157:1217-26.
68. **Pulak, R.** (2006). Techniques for analysis, sorting, and dispensing of *C. elegans* on the COPAS flow-sorting system. *Methods Mol Biol* 351:275-86.
69. **Qian, F., F. J. Germino, Y. Cai, X. Zhang, S. Somlo, and G. G. Germino.** (1997). PKD1 interacts with PKD2 through a probable coiled-coil domain. *Nat Genet* 16:179-83.
70. **Qian, Q., H. Du, B. F. King, S. Kumar, P. G. Dean, F. G. Cosio, and V. E. Torres.** (2008). Sirolimus reduces polycystic liver volume in ADPKD patients. *J Am Soc Nephrol* 19:631-8.
71. **Rosner, M., C. Fuchs, N. Siegel, A. Valli, and M. Hengstschlager.** (2009). Functional interaction of mammalian target of rapamycin complexes in regulating mammalian cell size and cell cycle. *Hum Mol Genet* 18:3298-310.
72. **Sancak, Y., T. R. Peterson, Y. D. Shaul, R. A. Lindquist, C. C. Thoreen, L. Bar-Peled, and D. M. Sabatini.** (2008). The Rag GTPases bind raptor and mediate amino acid signaling to mTORC1. *Science* 320:1496-501.
73. **Sandford, R., S. Mulroy, and L. Foggensteiner.** (1999). The polycystins: a novel class of membrane-associated proteins involved in renal cystic disease. *Cell Mol Life Sci* 56:567-79.
74. **Sarbassov, D. D., D. A. Guertin, S. M. Ali, and D. M. Sabatini.** (2005). Phosphorylation and regulation of Akt/PKB by the rictor-mTOR complex. *Science* 307:1098-101.
75. **Saucedo, L. J., and B. A. Edgar.** (2007). Filling out the Hippo pathway. *Nat Rev Mol Cell Biol* 8:613-21.
76. **Sheaffer, K. L., D. L. Updike, and S. E. Mango.** (2008). The Target of Rapamycin pathway antagonizes pha-4/FoxA to control development and aging. *Curr Biol* 18:1355-64.
77. **Shillingford, J. M., N. S. Murcia, C. H. Larson, S. H. Low, R. Hedgepeth, N. Brown, C. A. Flask, A. C. Novick, D. A. Goldfarb, A. Kramer-Zucker, G. Walz, K. B. Piontek, G. G. Germino, and T. Weimbs.** (2006). The mTOR pathway is regulated by polycystin-1, and its inhibition reverses renal cystogenesis in polycystic kidney disease. *Proc Natl Acad Sci U S A* 103:5466-71.
78. **Shillingford, J. M., K. B. Piontek, G. G. Germino, and T. Weimbs.** (2010). Rapamycin ameliorates PKD resulting from conditional inactivation of Pkd1. *J Am Soc Nephrol* 21:489-97.
79. **Simmer, F., C. Moorman, A. M. van der Linden, E. Kuijk, P. V. van den Berghe, R. S. Kamath, A. G. Fraser, J. Ahringer, and R. H. Plasterk.** (2003). Genome-wide RNAi of *C. elegans* using the hypersensitive rrf-3 strain reveals novel gene functions. *PLoS Biol* 1:E12.
80. **Simmer, F., M. Tijsterman, S. Parrish, S. P. Koushika, M. L. Nonet, A. Fire, J. Ahringer, and R. H. Plasterk.** (2002). Loss of the putative RNA-directed RNA polymerase RRF-3 makes *C. elegans* hypersensitive to RNAi. *Curr Biol* 12:1317-9.
81. **Soukas, A. A., E. A. Kane, C. E. Carr, J. A. Melo, and G. Ruvkun.** (2009). Rictor/TORC2 regulates fat metabolism, feeding, growth, and life span in *Caenorhabditis elegans*. *Genes Dev* 23:496-511.

82. **Spieth, J., G. Brooke, S. Kuersten, K. Lea, and T. Blumenthal.** (1993). Operons in *C. elegans*: polycistronic mRNA precursors are processed by trans-splicing of SL2 to downstream coding regions. *Cell* 73:521-32.
83. **Stiernagle, T.** (2006). Maintenance of *C. elegans*. . *WormBook*, ed. The *C. elegans* Research Community, WormBook, doi/10.1895/wormbook.1.101.1, <http://www.wormbook.org>.
84. **Sulston, J. E.** (1983). Neuronal cell lineages in the nematode *Caenorhabditis elegans*. *Cold Spring Harb Symp Quant Biol* 48 Pt 2:443-52.
85. **Sulston, J. E., and H. R. Horvitz.** (1977). Post-embryonic cell lineages of the nematode, *Caenorhabditis elegans*. *Dev Biol* 56:110-56.
86. **Syntichaki, P., K. Troulinaki, and N. Tavernarakis.** (2007). eIF4E function in somatic cells modulates ageing in *Caenorhabditis elegans*. *Nature* 445:922-6.
87. **Tao, Y., J. Kim, R. W. Schrier, and C. L. Edelstein.** (2005). Rapamycin markedly slows disease progression in a rat model of polycystic kidney disease. *J Am Soc Nephrol* 16:46-51.
88. **Thivierge, C., A. Kurbegovic, M. Couillard, R. Guillaume, O. Cote, and M. Trudel.** (2006). Overexpression of PKD1 causes polycystic kidney disease. *Mol Cell Biol* 26:1538-48.
89. **Timmons, L., and A. Fire.** (1998). Specific interference by ingested dsRNA. *Nature* 395:854.
90. **Torres, V. E., and P. C. Harris.** (2009). Autosomal dominant polycystic kidney disease: the last 3 years. *Kidney Int* 76:149-68.
91. **Toth, M. L., T. Sigmoid, E. Borsos, J. Barna, P. Erdelyi, K. Takacs-Vellai, L. Orosz, A. L. Kovacs, G. Csikos, M. Sass, and T. Vellai.** (2008). Longevity pathways converge on autophagy genes to regulate life span in *Caenorhabditis elegans*. *Autophagy* 4:330-8.
92. **Tsiokas, L., E. Kim, T. Arnould, V. P. Sukhatme, and G. Walz.** (1997). Homo- and heterodimeric interactions between the gene products of PKD1 and PKD2. *Proc Natl Acad Sci U S A* 94:6965-70.
93. **Vellai, T., K. Takacs-Vellai, Y. Zhang, A. L. Kovacs, L. Orosz, and F. Muller.** (2003). Genetics: influence of TOR kinase on lifespan in *C. elegans*. *Nature* 426:620.
94. **Wahl, P. R., A. L. Serra, M. Le Hir, K. D. Molle, M. N. Hall, and R. P. Wuthrich.** (2006). Inhibition of mTOR with sirolimus slows disease progression in Han:SPRD rats with autosomal dominant polycystic kidney disease (ADPKD). *Nephrol Dial Transplant* 21:598-604.
95. **Walz, G.** (2006). Therapeutic approaches in autosomal dominant polycystic kidney disease (ADPKD): is there light at the end of the tunnel? *Nephrol Dial Transplant* 21:1752-7.
96. **Wormatlas.** <http://www.wormatlas.org>.
97. **Wormbase.** <http://www.wormbase.org>.
98. **Wullschleger, S., R. Loewith, and M. N. Hall.** (2006). TOR signaling in growth and metabolism. *Cell* 124:471-84.
99. **Yang, Q., and K. L. Guan.** (2007). Expanding mTOR signaling. *Cell Res* 17:666-81.

100. **Yoder, B. K.** (2007). Role of primary cilia in the pathogenesis of polycystic kidney disease. *J Am Soc Nephrol* 18:1381-8.
101. **Yoder, B. K., X. Hou, and L. M. Guay-Woodford.** (2002). The polycystic kidney disease proteins, polycystin-1, polycystin-2, polaris, and cystin, are co-localized in renal cilia. *J Am Soc Nephrol* 13:2508-16.
102. **You, Y. J., J. Kim, D. M. Raizen, and L. Avery.** (2008). Insulin, cGMP, and TGF-beta signals regulate food intake and quiescence in *C. elegans*: a model for satiety. *Cell Metab* 7:249-57.
103. **Zorio, D. A., N. N. Cheng, T. Blumenthal, and J. Spieth.** (1994). Operons as a common form of chromosomal organization in *C. elegans*. *Nature* 372:270-2.

## 9. Acknowledgements

First of all I would like to thank Prof. Dr. Gerd Walz for the opportunity to work in his laboratory, providing me an invaluable environment for personal and professional development.

I would also like to thank my supervisor Dr. Elke Neumann-Haefelin for being my dedicated guide throughout these years, and for giving me continuous support and advice. Special thanks to Alexandra Schwierzok for the technical support and for sharing with me her enthusiasms and spirit. To Foteini Noutsou and Antje Thien, thank you for your motivation and friendship. And to the latest members of our 'worm group', Nicola Wanner and Vanessa Ruf, thank you for your help.

I am also very grateful to all other members of the Walz Lab for all the help provided and for creating a great working atmosphere. Special thanks to the 'Denkzelle' people and to all the other doctoral students for the great moments inside and outside the laboratory.

Furthermore, I would like to thank Prof. Dr. Ralf Baumeister and all the members of the Baumeister group for their help and collaboration.

I am also grateful to Prof. Dr. Hans-Georg Koch for reviewing my thesis.

To all my friends in Freiburg, thank you for their unconditional support and for being always there for me in good and bad moments. Special thanks to 'die Guntram' for becoming my German family.

And last but not least, I am deeply grateful to my family, especially to my parents: muchas gracias por vuestro apoyo y vuestros consejos en momentos de incertidumbre, y por brindarme la inestimable oportunidad de explorar otros horizontes.

## 10. Curriculum Vitae

Name	Raquel Guerola Segura
Place of birth	Sevilla, Spain
Date of birth	8th January 1983

### Education

2007-2010	Doctoral thesis in Prof. Dr. Walz Lab, department of Nephrology, University Hospital Freiburg.
2007	Degree in Medicine by the University of Sevilla.
2005-2006	Year abroad with an Erasmus scholarship in the Albert-Ludwig University of Freiburg.
2004	Beginning of the clinical studies in the University Hospital Nuestra Señora de Valme, Sevilla.
2002-2003	Member of the organizing committee of the 'VI Congress of physiology students' of the Faculty of Medicine, University of Sevilla.
2001	Beginning of medical degree studies in the Faculty of Medicine, University of Sevilla; beginning of the pre-clinical studies in the University Hospital Virgen Macarena, Sevilla.
1997-2001	Secondary education in I.E.S. Isbilya, Sevilla.
1996-1997	Primary education in C.P. Al-Andalus, Sevilla.
1986-1996	Primary education in C.P. Adriano, Sevilla.